Effect of Immobilized Chrysophsin-1 on *S. aureus*

A Major Qualifying Project Report

Submitted to the Faculty of

WORCESTER POLYTECHNIC INSTITUTE

In partial fulfillment of the requirements

for the Degree of Bachelor of Science

in the field of Chemical Engineering by

_____

Christopher Bannon

_____

Emily Skelton

_____

Kathryn Tongue

Date: April 17, 2013

Approved:

_____

Professor Terri A. Camesano, Advisor

Executive Summary

Food-borne illnesses and nosocomial infections are often the result of physical contact with surfaces that are contaminated with harmful bacteria. In 2011, it was estimated that approximately 48 million people were affected by food-borne illnesses; 120,000 were hospitalized and 3,000 people died (CDC 2011 Estimates: Findings 2012). Over the years, bacterial resistance to antibiotics has continued to increase (Costa, et al. 2011). Therefore, novel technologies are needed to prevent and treat bacterial infections.

One potential alternative to traditional antibiotics is the use of antimicrobial peptides (AMPs). Research has shown that it is harder for bacteria to adapt and become resistant to AMPs because of the ability of the peptide to target multiple sites on the membrane, allowing the peptide to kill the bacteria (Kulagina, et al. 2005). In addition to killing bacteria while in solution, AMPs have been shown to be effective in killing or limiting the growth of bacteria while immobilized on a substrate (Ivanov, et al. 2012). As such, attaching AMPs to a substrate to create an antimicrobial surface could drastically reduce the number of bacterial infections caused by contaminated biomedical devices and food processing equipment.

There are several ways to attach AMPs to surfaces, including the use of spacer molecules (Ivanov, et al. 2012). The effect of spacer length on AMP efficiency has been researched, but the effectiveness of the spacer may differ depending on whether the bacteria are gram-positive or gram-negative. This study investigated the specific relationship the use of a spacer molecule and AMP activity against gram-positive bacteria.

One method used to investigate the relationship between spacer length and AMP activity is the use of Quartz Crystal Microbalance with Dissipation monitoring (QCM-D). This technology has been used for gram-negative bacteria but has not yet been applied to gram-positive. Using this method, it was shown that chrysophsin-1 has an $82\pm11\%$ killing percentage of *E. coli* HB101 when it is covalently attached to a silicon dioxide surface via a polyethylene glycol-12 ($SM(PEG)_{12}$) linker. We hypothesized that for a $SM(PEG)_{12}$ spacer length, the killing percentage of gram-positive bacteria will also be approximately 80%. For our purpose, this methodology was applied to investigate the killing percentage that chrysophsin-1 has on gram-positive bacteria, specifically *S. aureus,* in comparison to gram-negative bacteria. To this end, our hypothesis was tested by using the QCM-D and a live/dead bacterial viability assay to investigate the killing percentage of *S. aureus* by chrysophsin-1 when this peptide is attached to a surface via a $SM(PEG)_{12}$ spacer molecule.

To test this hypothesis, the antimicrobial peptide chrysophsin-1 was attached to a SiO_2 surface via a flexible $SM(PEG)_{12}$ spacer molecule. To study the effect of this immobilization approach, the ability of the $SM(PEG)_{12}$ covalently immobilized peptide to kill *S. aureus* was compared to peptide that was physically adsorbed to the SiO_2 surface. For the covalently immobilized peptide, $SM(PEG)_{12}$ was bound to an amine-functionalized QCM-D crystal and modified chrysophsin-1 was bound to the $SM(PEG)_{12}$ linker.

The experimental results for both the physical adsorption of chrysophsin-1 and the adsorption via a $SM(PEG)_{12}$ are shown in the table below.

Comparison of changes in frequency, mass, and percent dead cells for the physically adsorbed peptide and peptide bound via a linker.

	Physically adsorbed peptide	Peptide bound through SM(PEG)$_{12}$ linker
Δf (hz) of peptide adsorption	10.0	71.2
Mass of peptide adsorbed (ng)	25.3	180
Percent of dead cells (*S. aureus*)	55 ± 14	39 ± 10

Despite having a greater degree chrysophsin-1 adsorption during the SM(PEG)$_{12}$ trials, it was found that the addition of the SM(PEG)$_{12}$ spacer decreased the killing percentage of *S. aureus*. It was expected that the killing percentage would have been much higher with the addition of the spacer molecule than when the peptide was physically adsorbed onto the surface. Since the killing percentage for the (SM)PEG$_{12}$/C-CHY1 system did not increase proportionally with the increase in mass compared to the physically adsorbed peptide, the binding of the C-CHY1 to the surface via the linker molecule may be inhibiting the ability of the peptide to disrupt the bacterial membrane.

One possible hypothesis to explain the decreased killing percentage for both the physically adsorbed peptide and the covalently bound chrysophsin-1 with the gram-positive *S. aureus* bacteria could be the difference in the cell wall structure of the gram-positive bacteria. The thick peptidoglycan layer may not allow the peptide to interact with the bacterial cell membrane in such a way that the AMP can effectively cause cell death. The concentration of peptide present may not be sufficient to achieve the 80-90% killing that has been previously observed (Ivanov, et al. 2012). Additional linker molecule lengths should be studied to determine if a longer linker molecule could allow the peptide to more effectively kill gram-positive bacteria.

Additionally, the level or uniformity of saturation of the peptide on the surface was not characterized. During the experimentation, a variation in killing percentage was observed between different locations on each crystal. This is likely due to the crystal surface not being uniformly covered with peptide. Future work could include further characterizing the density and uniformity of the peptide adsorption on the crystal surface and investigate potential correlations between amount of peptide on the surface and the antimicrobial efficacy of the peptide.

In future experiments, the effect of repeatedly freezing and thawing of the peptide should be studied. This process could potentially have an effect on the ability of the peptide to bind as well as the antibacterial properties of the peptide. Additionally, previous data had manually counted the number of live and dead cells on the crystal surface, while images from this study were counted using ImageJ software (Ivanov, et al. 2012). This may have had an effect on the calculated killing percentages since there may have been inconsistencies in exactly what was counted as a cell. The experiments with gram-negative bacteria should be repeated and the images analyzed with ImageJ software to determine if the counting procedure had any effect on the calculated killing percentage. By doing so, more accurate data would be collected, which would lead to a clearer conclusion about the ability of tethered AMPs to kill gram-positive bacteria.

Acknowledgements

We would like begin by thanking our advisor, Professor Terri A. Camesano for the opportunity to work on this project. It has been an interesting and rewarding experience.

We would also like to thank the graduate students of the Camesano lab for their guidance and advice. Special thanks to Todd Alexander for all of his assistance with this methodology, including the QCM-D and microscopy.

Finally, thank you to Professor Luis Vidali for his assistance with the ImageJ software.

Table of Contents

List of Figures

List of Tables

1. Introduction

Food-borne illnesses and nosocomial infections are often the result of physical contact with surfaces that are contaminated with harmful bacteria. In 2011, it was estimated that approximately 48 million people were affected by food-borne illnesses; 120,000 were hospitalized and 3,000 people died (CDC 2011 Estimates: Findings 2012). Over the years, bacterial resistance to antibiotics has continued to increase (Costa, et al. 2011). Therefore, novel technologies are needed to prevent and treat bacterial infections.

One potential alternative to traditional antibiotics is the use of antimicrobial peptides (AMPs). AMPs are naturally occurring proteins that are part of the innate defense system of many organisms, including plants, fish, and mammals, and protect the organism from microbial infection (Arcidiacono, et al. 2008). Research has shown that it is harder for bacteria to adapt and become resistant to AMPs because of the ability of the peptide to target multiple sites on the membrane, allowing the AMP to kill the bacteria (Kulagina, et al. 2005). In addition to killing bacteria while in solution, AMPs have been shown to be effective in killing or limiting the growth of bacteria while attached to a substrate (Ivanov, et al. 2012). As such, attaching AMPs to a substrate to create an antimicrobial surface could drastically reduce the number of bacterial infections caused by contaminated biomedical devices and food processing equipment.

There are several ways to attach AMPs to surfaces, including the use of spacer molecules (Ivanov, et al. 2012). The effect of spacer length on AMP efficiency has been researched and it was found that the spacer's effectiveness may differ depending on whether the bacteria are gram-positive or gram-negative. This study investigated the specific relationship between spacer lengths and AMP activity against gram-positive bacteria.

1.1. Hypothesis

One method used to investigate the relationship between spacer length and AMP activity is the use of Quartz Crystal Microbalance with Dissipation monitoring. This technology has been used for gram-negative bacteria but has not yet been applied to gram-positive. Using this method, it has been shown that chrysophsin-1 has an $82 \pm 11\%$ killing percentage of *E. coli* HB101 when it is covalently attached to a silicon dioxide surface via a polyethylene glycol $(SM(PEG)_{12})$ linker. We hypothesized that for a $SM(PEG)_{12}$ spacer length, the killing percentage of gram-positive bacteria would also be approximately 80%. For our purpose, this methodology was applied to investigate the killing percentage that chrysophsin-1 has on gram-positive bacteria, specifically *S. aureus,* in comparison to gram-negative bacteria. To this end, our hypothesis was tested by using the QCM-D and a live/dead bacterial viability assay to investigate the killing percentage of *S. aureus* by chrysophsin-1 when this peptide is attached to a surface via a $SM(PEG)_{12}$ spacer molecule.

2. Literature Review

2.1. AMPs: Types and Mechanism

AMPs are commonly found in nature in a variety of organisms. These peptides are distinguished by their small size and amphipathic nature. Their high structural stability and ability to refold after exposure to heat (Ivanov, et al. 2012) make them promising candidates for antimicrobial surfaces, which would enable them to be used on surfaces that require autoclaving (Arcidiacono, et al. 2008). AMPs can be classified by their secondary structure, which is often a beta sheet or an alpha helical formation. It has been found that alpha helical AMPs can adopt two different structures: a globular structure in solution and an alpha helical amphipathic structure when bound to a target (Uzarski, et al. 2008).

Both cationic and anionic AMPs are present in nature, but more research has been focused on cationic AMPs and their interactions with bacteria. Research shows that the net positive charge of cationic AMPs causes a strong attraction to some bacteria with a net negative charge on their surface (Cronin and Kadilak 2008). Some of the main criteria that may need to be considered when analyzing binding of AMPs are the concentration of the microbe they are attacking and the charge and hydrophobicity of both the AMP and the microbe (Ivanov, et al. 2012). AMPs vary in size and structure and their activity depends on the charge, composition, and concentration of the bacterial cell membrane. The complexity of these interactions has led to the conclusion that there is not one specific mechanism for how bacteria are killed by AMPs (Wang, et al. 2011). Though research has been done with regard to the mechanism of action of AMPs against gram-negative bacteria, there are several plausible mechanisms for this process.

2.2. Mechanisms of Killing

Three mechanisms of action have been proposed for the AMP/gram-negative bacteria interaction: the carpet model, the barrel-stave model, and the toroidal model. Each of these three models shows that the AMP attaches to the bacterial cell membrane through electrostatic interactions and causes the cells to lyse due to a disruption in the membrane. There is speculation regarding how the membrane is broken and whether the AMP also attacks intracellular components (Strauss, et al. 2010).

The carpet model states that the AMP aligns parallel to the bacterial cell membrane covering the length of the cell, surrounding the lipids, and disintegrating the membrane. This forces micelle aggregates to break away from the membrane and form a pore (Wang, et al. 2011, Strauss, et al. 2010). As shown in Figure 1 below, the AMP attaches to the lipopolysaccharide membrane of the gram-negative bacterial cells and breaks it apart, forming a pore through which foreign components can enter and disrupting the osmotic equilibrium of the cell (Brogden 2005).
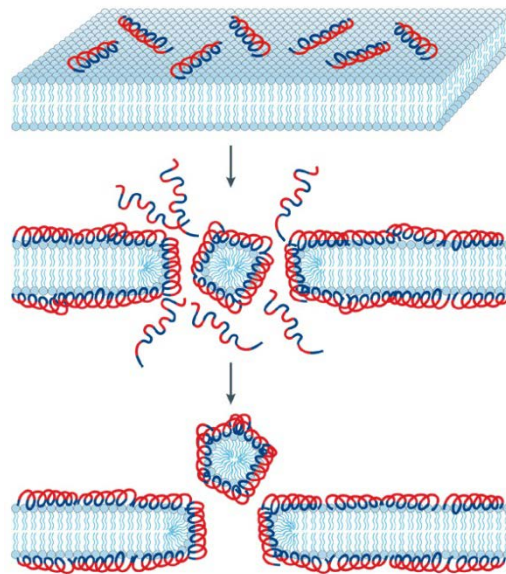

Figure 1. Carpet model mechanism of killing bacterial cells (Brogden 2005).

Another proposed mechanism is the barrel-stave model. The main difference between the carpet and barrel-stave models is that the AMP inserts itself into the membrane, rather than breaking off micelles from the membrane. The AMP aligns itself perpendicular to the bacterial membrane and enters the cell in that orientation. It is then able to form a cylindrical pore spanning the entire width of the membrane (Strauss, et al. 2010). Similar to the carpet model, this pore will allow objects in and out of the cell, causing cell death.

The toroidal model is very similar to the barrel-stave model, but differs in the orientation of the lipid bilayer with respect to the AMP. In the toroidal model, the lipid head groups of the lipopolysaccharide membrane are always in contact with the AMP, even as the AMP inserts into the membrane. This process results in a pore lined with both AMP molecules and lipid head groups. In the barrel-stave model, the AMP enters the membrane but does not take the lipid head groups of the bilayer with it, resulting in a transmembrane pore lined only with AMP molecules. This concept is illustrated below in Figure 2.
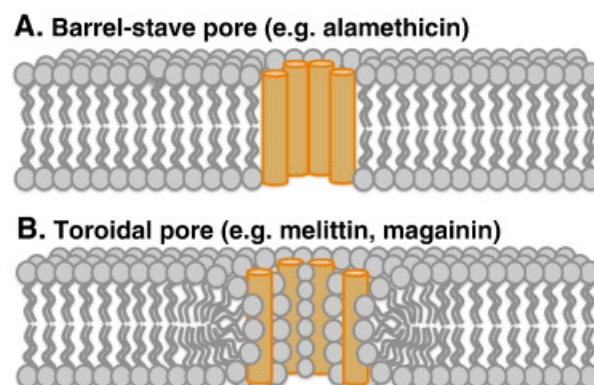

Figure 2. Barrel-stave and toroidal pore method of killing bacterial cells (Westphal, et al. 2011).

2.3. Gram-Positive versus Gram-Negative Bacteria

AMPs have been shown to exhibit antimicrobial activity against both gram-positive and gram-negative bacteria. Some studies suggest that AMPs have a lower activity against and an unknown mechanism for gram-positive bacteria (Strauss, et al. 2010). Gram-negative bacteria have been studied more closely because of the known electrostatic interaction between the lipopolysaccharide bacterial membrane and AMPs. The interactions between AMPs and the peptidoglycan layer surrounding gram-positive bacteria, however, are not as well understood.

Figure 3 depicts some of the main differences between the structure of gram-negative and gram-positive bacteria. The cell wall of the gram-negative bacteria is more complex than that of the gram-positive bacteria. Gram-positive bacteria have a cell wall made almost entirely of a thick peptidoglycan layer. Gram-negative bacteria have a lipopolysaccharide membrane and a phospholipid bilayer on either side of the cell wall, while the gram-positive only have the phospholipid bilayer on one side of the cell wall (Baron 1996).
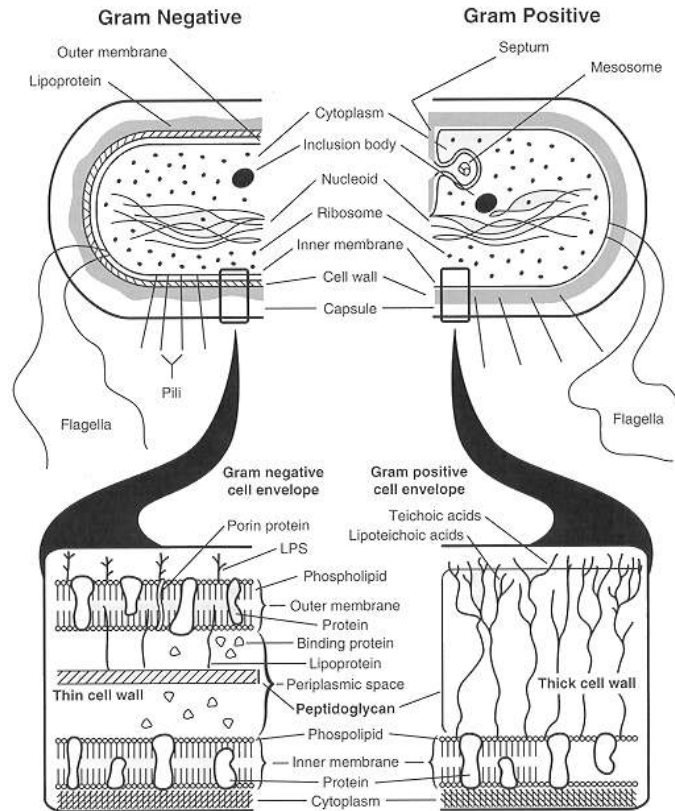
Figure 3. Comparison of the structure of gram-negative and gram-positive bacteria (Baron 1996).

The lipopolysaccharide head groups on the outer part of the gram-negative bacteria have a negative charge, which gives the bacteria a high affinity for cationic AMPs. The charge interaction at the outer membrane plays a large role in the binding and possible deactivation of the bacteria (Cronin and Kadilak 2008). All methods of killing mentioned in Section 2.2 were in regards to gram-negative bacteria, and little research has been done on the mechanism of how AMPs kill gram-positive bacteria. It is known that AMPs kill both gram-negative and gram-positive bacteria, but there remains discussion on the mechanism of AMPs killing gram-positive bacteria, particularly with respect to tethered AMPs.

2.4. Peptide Immobilization

Studies with various goals have been conducted involving the attachment of AMPs to surfaces. The specific aims of each study dictated the peptide sequence, substrate, immobilization strategy, control of AMP orientation, and/or bacterial strain that was investigated (Costa, et al. 2011). Several surfaces have been used as substrates onto which the peptides have been immobilized, including various resins, contact lenses, glass, microtiter plates, titanium, and gold (Costa, et al. 2011, Ivanov, et al. 2012, Uzarski, et al. 2008, Gregory and Mello 2005). Attachment strategies also differ from study to study. Some have used physical adsorption of the peptide to the surface; however, this strategy may limit the antibacterial activity of the peptide (Ivanov, et al. 2012). AMPs have been synthesized directly onto surfaces using methods such as standard solid-phase peptide synthesis, which provides the greatest control over peptide orientation (Costa, et al. 2011, Haynie, Crum and Doele 1995). Additionally, AMPs have been immobilized to substrates using biotin-avidin chemistry (Kulagina, et al. 2005). Covalent immobilization techniques are common and involve either the functionalization of the surface or the peptide in order to facilitate this attachment. Examples of the chemistries that have been employed include amide bonds, disulfide bridges, binding thiol groups to maleimide or epoxide modified surfaces, azide linkers, and Huisgen 1,3 dipolar cycloaddition ('click' reactions) (Costa, et al. 2011, Ivanov, et al. 2012, Chen, et al. 2009).

In order to covalently attach AMPs to substrates, many studies used functionalized surfaces to provide carboxyl or other reactive groups with which the peptide can bond. Another common approach is to functionalize the peptide to provide a designated site for binding. This helps to control the peptide orientation while it is bound to the substrate (Costa, et al. 2011, Arcidiacono, et al. 2008). An engineered C-terminal cysteine residue added to a peptide has been

used in several studies. This approach is particularly useful for specific AMPs, such as magainin I, which does not have naturally occurring cysteine residues. This allows the peptide to be attached to the surface in a specific orientation since there is only one binding site available on the peptide (Glinel, et al. 2009). Another approach is to functionalize the substrate with polymer spacers. The spacers may allow the peptide to move more freely and act more effectively against bacteria. However, the relationship between spacer length and bactericidal activity is not clear.

Spacer molecules have also been used between the substrate and the peptide itself. Haynie, et al. used an ethylenediamine (two carbon) spacer and a hexamethylenediamide (six carbon) spacer for attaching the peptide to the insoluble resin used as the substrate. In this study, several peptides were analyzed and no significant differences were observed between the different spacer lengths in terms of the bactericidal activity of the peptides. The study concluded that one of the most critical factors to bactericidal activity was that the peptide retains its amphipathic properties despite immobilization (Haynie, Crum and Doele 1995). Another study has used polymer brushes and a PMPI heterolinker to connect the antimicrobial peptide, specifically magainin I, to surfaces (Glinel, et al. 2009). Bagheri, et al. studied the effect of immobilization and spacer length on AMP activity with *E. coli* (gram-negative) and *B. subtilis* (gram-positive) bacteria. Generally, this study found that longer spacer lengths correlate with higher bacterial killing (Bagheri, Beyermann and Dathe 2009). In order to further clarify this relationship, additional data should be generated regarding the interactions of tethered AMPs and bacteria.

2.5. QCM-D

One way to measure the effects that AMPs have on cell membranes is through a technique known as Quartz Crystal Microbalance with Dissipation monitoring (QCM-D). This

technique correlates changes in mass and physical structure of material on a quartz crystal with changes in frequency and dissipation of the crystal. The QCM-D experimental process begins by oscillating the crystal at a known frequency. An aqueous solution containing the desired material is then distributed through the instrument and comes into contact with the crystal, where the material is then deposited on its surface. As the mass of the material on the crystal is increased, the frequency of the oscillation of the crystal decreases. Conversely, a decrease in mass is represented by an increase in the frequency. This phenomenon is characterized through the Sauerbrey equation (Q-Sense, Inc.):

$$\Delta m = \frac{-C\Delta f}{n}$$ (1)

In this equation, C represents the mass sensitivity constant, Δf represents the change in the frequency of the crystal, and n represents the overtone number.

Changes in mass are also quantified by calculating the dissipation of the crystal, which measures the rate of energy loss from the system when the oscillation cycle of the crystal is abruptly stopped. Dissipation is further defined as (Q-Sense, Inc.):

$$D = \frac{E_{lost}}{2\pi E_{stored}}$$ (2)

As measured by the QCM-D, the dissipation of the system increases as mass is increased, and decreases as mass is decreased. In addition to enabling mass calculations, determining the dissipation of the system gives insight into the structure of the molecular layer that is attached to the crystal: a soft layer will result in greater dissipative losses than a rigid layer (Q-Sense, Inc.).

The vast amount of data that is obtained through QCM-D experiments is invaluable in the AMP experimental field.

QCM-D has been used to monitor the immobilization of AMPs on a surface. The density of the AMP adsorption can be calculated using the QCM-D experimental data. Dissipation measurements also make it possible to make assumptions about the configuration and orientation of the AMPs on the surface, which can be useful for comparing various surface adsorption methods and AMP spacer lengths (Ivanov, et al. 2012).

Additionally, the QCM-D has been used to study the various methods by which AMPs disrupt cell membranes. Wang, et al. used QCM-D to study the adsorption of AMPs onto lipid membranes. During the experimental process, an initial decrease in frequency was observed when the AMPs came into contact with the membrane, signifying the adsorption of the AMPs. Over time, however, an increase in the frequency of the crystal was observed. This indicated that the AMPs formed pores in the membrane, which led to an eventual removal of mass from the crystal. Changes in the dissipation were also closely monitored during this experimental process, as these changes shed light onto the structure and orientation of the AMPs as they adsorbed onto the crystal. By closely analyzing this data, Wang et al. were able to propose detailed mechanisms for the destruction of cell membranes through AMP exposure.

Similar experimental procedures involving the QCM-D have been used to study the membrane interactions between living cells and the surface of the SiO_2 quartz crystal. Elwing, et al. explored the idea of using the QCM-D to monitor the effects that variations in the ionic strength of hydrophobic and hydrophilic crystal surfaces had on *E.coli* growth. By observing the changes in frequency and dissipation of the crystal, changes in cell growth were able to be

monitored and were correlated to variations in the surface properties of the crystal (Elwing, Hermansson and Otto 1999). Similar techniques for monitoring cell growth have been used to investigate the effects of AMP coated surfaces on bacterial growth (Ivanov, et al. 2012). As exemplified in these publications, QCM-D is capable of accurately measuring the adhesion and growth of cells on various surfaces, which is instrumental for studying the interactions between AMPs and living cells.

2.6. Determining Cell Death through a Fluorescent Live/Dead Assay

To further understand the bactericidal properties of AMPs, a live/dead assay can be used in conjunction with QCM-D experimental procedures. Live/dead assays use two fluorescent dyes that allow the number of live and dead cells to be counted when viewed under a fluorescent microscope. Two dyes are used in this assay, SYTO 9® and propidium iodide. Both dyes have relatively low fluorescence when they are not in contact with nucleic acids and display a 30-40 fold increase in fluorescence when bound to nucleic acids (Molecular Probes, Propidium Iodide Nucleic Acid Stain 2006, Molecular Probes, SYTO(R) Green-Fluorescent Nucleic Acid Stains 2011). SYTO 9® dye is a green dye that stains all cells since it is able to permeate the cell membrane of various cell types, including gram-positive and gram-negative bacteria. Propidium iodide is a red dye that stains only cells with disrupted cell membranes because it is not able to pass through intact cell membranes (Brana, Benham and Sundstrom 2002). The green fluorescence of SYTO 9® diminishes in those cells where propidium iodide is also present, leaving these cells displaying primarily red fluorescence (Berney, et al. 2007).

After staining a sample with both dyes, the sample can be viewed with a fluorescence microscope under appropriate filters. The assumption that only live cells will fluoresce green and only dead cells will fluoresce red may not be entirely correct since dead cells could potentially

still have intact membranes, depending on the mechanism of cell death (Berney, et al. 2007).

However, for the purposes of this study, cells that are red are considered 'dead' and cells that are

green are considered 'live'. This type of assay is useful for quantifying cell death due to the

disintegration of the bacterial cell membrane, which may be caused by AMPs.

2.7. Conclusion

The study of the interactions between AMPs and bacteria could lead to important

advances in the treatment and prevention of infections. The attachment of AMPs to surfaces

would further improve the utility of these molecules. Using QCM-D and fluorescent live/dead

assays could allow for the interactions between tethered AMPs and gram-positive bacteria to be

better understood.

3. Methodology

The antimicrobial peptide chrysophsin-1 (CHY1) was attached to a SiO_2 surface via a flexible $SM(PEG)_{12}$ spacer molecule. To study the effect of this immobilization approach, the ability of the $SM(PEG)_{12}$ covalently immobilized peptide to kill *S. aureus* was compared to peptide that was physically adsorbed to the SiO_2 surface. For the covalently immobilized peptide, $SM(PEG)_{12}$ was bound to an amine-functionalized QCM-D crystal and modified chrysophsin-1 was bound to the $SM(PEG)_{12}$ linker (Figure 4).
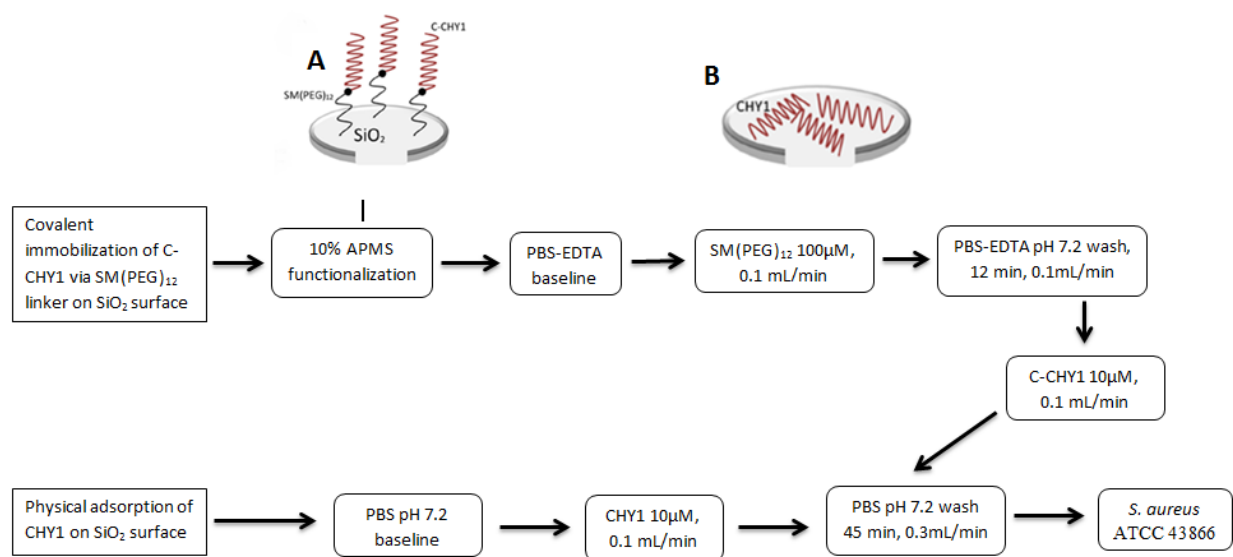
Figure 4. Diagram of peptide immobilization (top; not drawn to scale) and overview of immobilization procedure (bottom).
Chrysophsin-1(CHY1) was attached to the SiO_2 surface via a flexible $SM(PEG)_{12}$ linker molecule (A). To isolate the effect of the flexible linker molecule, CHY1 was physically adsorbed to the SiO_2 surface (B). In (A), an amine-functionalized SiO_2 QCM-D crystal is coated with $SM(PEG)_{12}$. The modified chrysophsin-1 is then bound to the linker molecule. In (B), the chrysophsin-1 is physically adsorbed directly to the SiO_2 QCM-D crystal.

3.1. Bacterial Culture and Harvesting

Staphylococcus aureus (ATCC 43866) was cultured in 50mL of 30g/L Tryptic Soy Broth, incubated at a temperature of 37°C, and placed on a shaker plate for approximately 9 hours in order to reach the late log phase of bacterial growth. The late log phase was determined by measuring the optical density of the *S. aureus* culture over a 16-hour period of time. The

14

obtained *S. aureus* growth curve is shown in Appendix A. To prepare the *S. aureus*, 10mL of the

bacteria in solution was washed twice with 0.01M phosphate buffered saline (PBS) pH7.2 by

centrifugation for 10 minutes at 2,000xg. After washing, the bacteria were diluted 100-fold.

3.2. Crystal Preparation

Q-Sense SiO_2 crystals (Biolin Scientific, Sweden) were cleaned in the Q-Sense E4 Quartz

Crystal Microbalance with Dissipation (QCM-D) chambers using 2.5mL of ethanol, 2.5mL of DI

water, 2.5mL of 2% sodium dodecyl sulfate (SDS), and 2.5 mL of DI water while at a

temperature of 40°C and a flow rate of 0.3 mL/min. All volumes are given on a per chamber

basis. The crystals were further cleaned by exposing them to an SPI Supplies Plasma Prep II

oxygen plasma cleaner for 2 minutes. Solutions of 0.01M phosphate buffered saline (PBS) and

phosphate buffered saline with 1 mM ethylenediaminetetraacetic acid (PBS-EDTA) were then

prepared at a pH of 7.2 and sonicated for 30 minutes to remove any gas from the solution.

Crystals to be used with spacer molecules were functionalized by incubation in a 10% (3-

aminopropyl) trimethoxysilane, 90% methanol solution for 20 minutes. Following the

incubation, each crystal was rinsed with methanol and water and dried with nitrogen.

3.3. Quartz Crystal Microbalance with Dissipation Monitoring

The 1st through 11th overtones were calibrated for each QCM-D chamber before the

buffer was introduced.

3.3.1. Physically Adsorbed Peptide

After the crystals were cleaned, PBS was flowed over the crystals at a flow rate of

0.1mL/min until a baseline was established. After establishing a baseline, 1.25mL of

chrysophsin-1 (CHY1) was flowed through all chambers and incubated for 30 minutes.

After incubation with the peptide, chambers were rinsed for 45 minutes with PBS pH 7.2 at a flow rate of 0.3 mL/min in order to remove peptide that was not strongly bound or adsorbed to the surface. After the rinse, 2.5mL of the 100-fold dilution of *S. aureus* were flowed through each chamber at 0.1mL/min, incubated for 1 hour. Following the incubation, the chambers were rinsed with 2.5mL of PBS pH 7.2.

3.3.2. Peptide with SM(PEG)$_{12}$ Spacer Molecule

PBS-EDTA was flowed over the functionalized crystals at a flow rate of 0.1 mL/min until a baseline was reached. Then 1 mL of 100 µM succinimidyl-[(N-maleimidopropionamido)-dodecaethyleneglycol] ester (SM(PEG)$_{12}$) solution was flowed through the QCM-D chambers and incubated for 30 minutes. Following this incubation, 1.25 mL of chrysophsin-1 with a modified N-terminal cysteine residue (C-CHY1) was flowed through the chambers and incubated for 30 minutes. Following this incubation with peptide, chambers were treated rinsed, and bacterial was introduced to the system and rinsed again as described in Section 3.3.1.

3.4. Bacterial Viability

After the final PBS rinse, the crystals were prepared for the fluorescent live/dead assay to determine the numbers of live and dead cells. For each crystal, 6 µL of each the Styo9® and propidium iodide dyes were added to 2 mL of 0.85% NaCl solution. Each crystal was placed in the diluted dye solution and incubated for 15 minutes. The crystals were then rinsed by removing it from the dye solution and placing it in 1 mL of 0.85% NaCL solution. Before imaging, the crystal was moved to a second rinse of 1 mL of 0.85% NaCl solution. A minimum of five locations per crystal were imaged using FITC and Texas Red filters with a Nikon Eclipse E400 fluorescence microscope. As many locations were imaged as possible before photobleaching was observed. Cells from each image were counted using ImageJ software. The color channels were

split using ImageJ and only the red or green channel, respectively, was analyzed. The threshold was set using the Max Entropy setting. The particle size was set to 8-150 square pixels and the circularity was set to 0.85-1.00. These settings were intended to simulate which cells would be counted on each crystal if the cells were to be counted manually.

4. Results

4.1. Characterization of Peptide and Bacterial Adsorption

4.1.1. Physical Adsorption of Chrysophsin-1

In order to isolate the effects of the SM(PEG)$_{12}$ spacer molecule, data was collected that demonstrated the antimicrobial activity of physically adsorbed chrysophsin-1. QCM-D was used to monitor the adsorption of the peptide to the SiO$_2$ surface. Changes in the frequency (Δf) and dissipation (ΔD) of the crystal were monitored throughout the experiment (Figure 5). Data was collected for ten replicates.
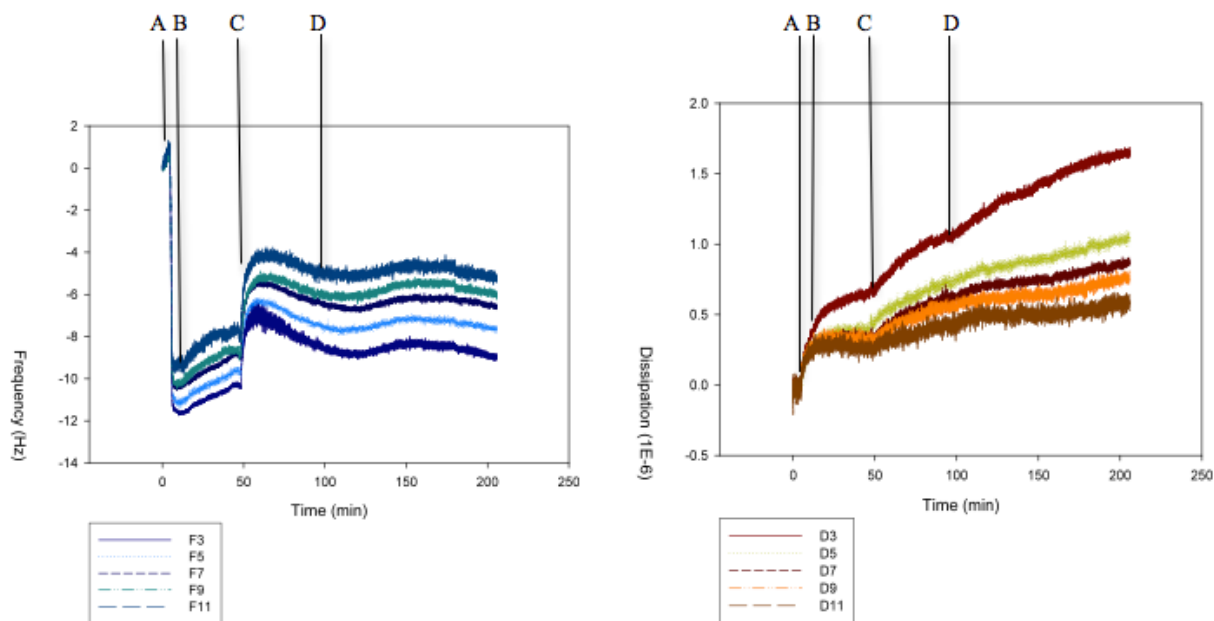
Figure 5. QCM-D data for physically adsorbed chrysophsin-1.
Dissipation (left) and frequency (right) for the 3rd through 11th overtones. At point A, chrysophsin-1 was introduced to the QCM-D chamber. Point B indicates the point at which CHY1 stopped flowing and began incubation. At point C, the crystals were rinsed with PBS. *S. aureus* was flowed through the chambers at Point D. A frequency decrease of approximately 10 hertz was observed for the adsorption of CHY1. Some of the peptide was removed from the surface when rinsed with PBS. Dissipation steeply with the introduction of the CHY1 and continued to increase at a slower rate throughout the remainder of the procedure. Dissipation increased most in the third overtone, indicating that the film was less rigid further from the surface of the crystal. The data shown is one of ten replicates. Dissipation and frequency changes for each trial are shown in Appendix B.

There was a substantial decrease in frequency when the chrysophsin-1 (CHY1) was flowed over the surface of the crystal. This signified the adsorption of the peptide onto the crystal. While the Δf ranged from 7 to 12 Hz, an average Δf of approximately 10.0 Hz was obtained for the physical adsorption of CHY1 onto the SiO_2 surface, based on data from the 7th overtone. The PBS rinse following the incubation of the peptide removed some of the CHY1 from the surface, as demonstrated by the increased frequency of the crystal. A decrease in frequency between 0.1 and 0.6 Hz, with an average of ~0.32 Hz, was then observed for the 7th overtone as *S. aureus* was flowed over the crystal, which confirmed the adsorption of the bacteria to the crystal surface. These phenomena are similar to those observed by Ivanov. et al in their efforts to physically adsorb CHY1 to a SiO_2 surface. Further data comparing the change in frequency for each overtone due to peptide and bacterial adsorption are shown in Appendix C.

The mass of the CHY1 and *S. aureus* that was physically adsorbed to the SiO_2 surface was determined using the Sauerbrey Equation (Equation 1) and a mass sensitivity constant of 17.7 ng Hz^{-1} cm^{-2}. From this equation, it was calculated that an average mass 24.0 ng of CHY1 and 2.34 ng of *S. aureus* adsorbed to the crystal surface during these trials.

The frequency increases at a higher rate than the dissipation during the physical adsorption of the CHY1 onto the SiO_2 surface (Figure 6). This slight decrease in dissipation implies that the CHY1 formed a relatively rigid, inflexible layer on the crystal. The curve begins to decrease as *S. aureus* is flowed through the QCM-D chambers, signifying that the dissipation is increasing at a higher rate than the frequency, thereby forming a soft, flexible layer on the crystal surface when compared to the peptide layer.
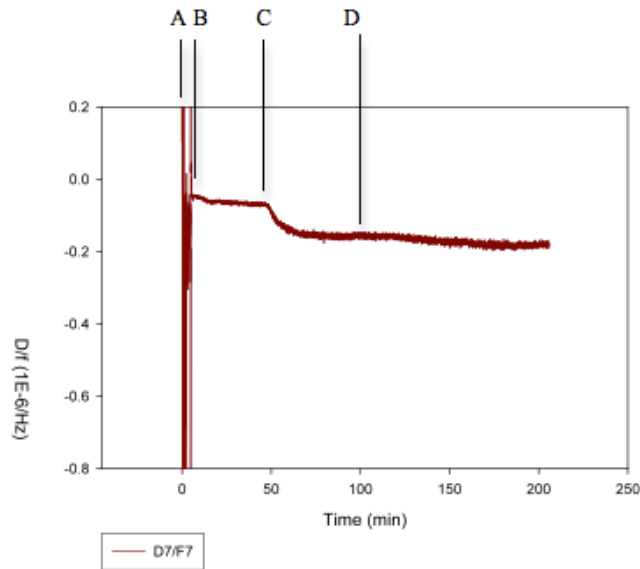
Figure 6. Variation of the dissipation to frequency ratio over time during the physical adsorption of CHY1.
Data shown for the 7th overtone. At point A, Chrysophsin-1 was introduced to the QCM-D chamber. Point B indicates the point at which CHY1 stopped flowing and began incubation. At point C, the crystals were rinsed with PBS. *S. aureus* was flowed through the chambers at Point D. The dissipation change to frequency change ratio demonstrates that the film on the crystal becomes less rigid as the mass adsorbs to the surface of the crystal. Compared to when the CHY1 was introduced, the change in this ratio was much less significant when bacteria were introduced to the system.

4.1.2. Covalent Attachment of Chrysophsin-1 through an SM(PEG)$_{12}$ Spacer Molecule

QCM-D was also used to determine how the SM(PEG)$_{12}$ spacer molecule affected the

killing percentage of *S. aureus*. Changes in frequency and dissipation were quantitatively

measured throughout the experiment (Figure 7).
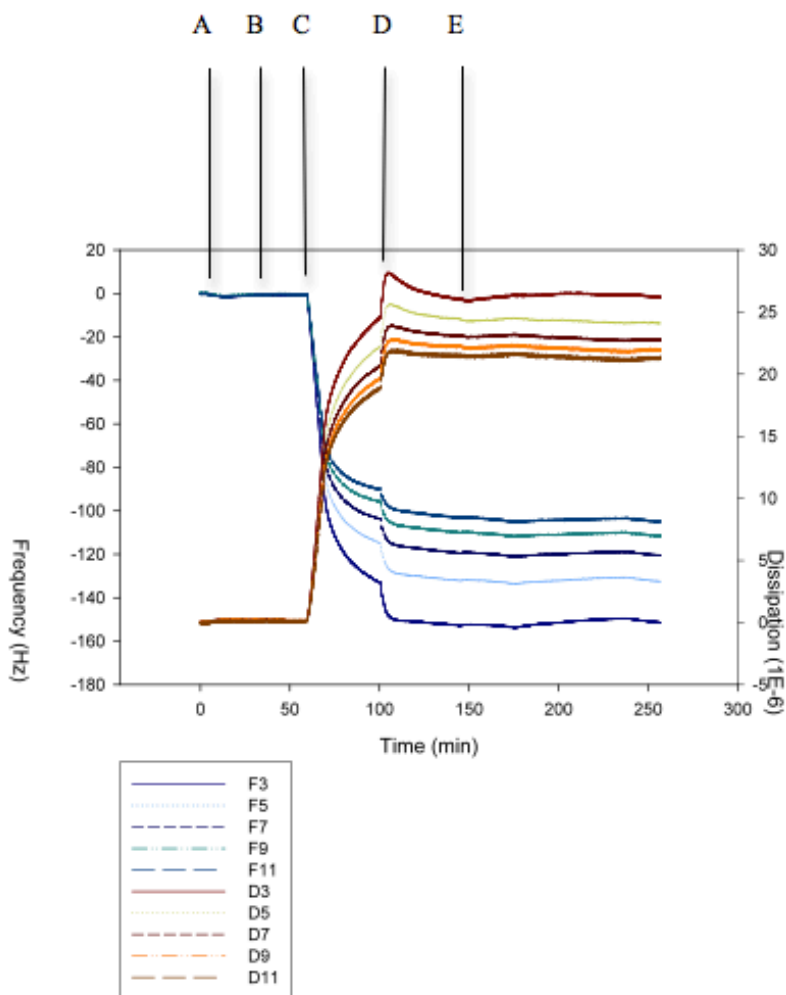
Figure 7. Δf and ΔD measured with QCM-D for SM(PEG)$_{12}$, C-Chrysophsin-1, and *S. aureus* adsorption onto the SiO$_2$ surface.
At point A, SM(PEG)$_{12}$ was flowed over the QCM-D chambers. The chambers were then rinsed with PBS-EDTA (Point B) prior to introducing C-CHY1 (Point C). Point D indicates the point at which the crystals were rinsed with PBS. At point E, *S. aureus* was flowed into the chambers. Significant frequency decreases were observed with the introduction of peptide. Additional peptide that had been in the tubing was adsorbed when the rinse began, indicating that the surface was not saturated. Frequency and dissipation changes for each trial are shown in Appendix B.

Small decreases in frequency, proportional to the mass of the adsorbed linker, were observed as the SM(PEG)$_{12}$ linker was flowed over the SiO$_2$ surface. The flow of the modified chrysophsin-1 (C-CHY1) after the adsorption of the SM(PEG)$_{12}$ led to rapid frequency changes, varying from 50 to 90 Hz. An average Δf for the 7th overtone of approximately 71 Hz was measured for the binding of the C-CHY1 to the linker. This demonstrates that the spacer

molecule effectively increases the attachment of the peptide to the surface when compared to physical adsorption. The beginning of PBS rinse following the C-CHY1 likely introduced residual peptide that had been in the inlet tubing of the QCM-D during the incubation. This caused an additional decrease in frequency at the beginning of the rinse as the C-CHY1 adsorbed to the surface. Following the PBS rinse, the *S. aureus* was flowed over the crystal, resulting in a Δf of approximately 1.3 Hz for the 7th overtone. Further data regarding the change in frequency due to both peptide binding and *S. aureus* adsorption are shown in Appendix C.

The mass of the C-CHY1 and *S. aureus* that adsorbed to the SiO_2 surface in the presence of the SM(PEG)$_{12}$ linker was also calculated through the Sauerbrey Equation. Using this equation, it was determined that an average mass of 145 ng of C-CHY1 and 1.79 ng of *S. aureus* attached to the crystal surface during these trials.
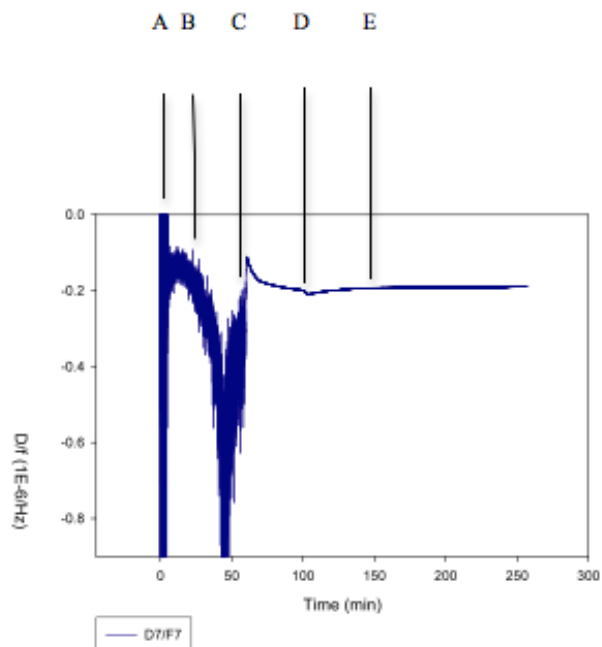
Figure 8. Variation of the dissipation to frequency ratio over time during the adsorption of SM(PEG)$_{12}$, CCHY1, and *S. aureus* onto the SiO$_2$ surface.
Dissipation change to frequency change ratio is shown for the 7th overtone. At point A, SM(PEG)$_{12}$ was flowed over the QCM-D chambers. The chambers were then rinsed with PBS-EDTA (Point B) prior to introducing C-CHY1 (Point C).

Point D indicates the point at which the crystals were rinsed with PBS. At point E, *S. aureus* was flowed into the chambers. The frequency increases much more quickly than the dissipation during the peptide adsorption, both when the peptide is first introduced and when additional peptide adsorbs at the beginning of the rinse.

Observation of the dissipation changes in the SiO_2 crystal throughout the experiment was important for understanding the orientation of the $SM(PEG)_{12}$, C-CHY1, and *S. aureus*. The slope of the dissipation to frequency curve increases rapidly as the $SM(PEG)_{12}$ is adsorbed. Since the frequency is increasing at a much higher rate than the dissipation during this period, it is shown that the $SM(PEG)_{12}$ formed a rigid, inflexible layer on the SiO_2 crystal. This period is followed by a sharp decrease in the dissipation to frequency ratio as the C-CHY1 is flowed through the QCM-D chambers. The decreased slope of the curve implies that the dissipation increased faster than the frequency, thereby suggesting that the C-CHY1 formed a soft layer on the surface. This implies that the C-CHY1 was in an upright position as it covalently bonded to the linker. The positive slope observed after the adsorption of the C-CHY1 is a result of the peptide removal during the PBS rinse. As shown, the flow of *S. aureus* over the surface following the PBS rinse indicates that the dissipation once again increased at a higher rate than the frequency, leading to the formation of a soft, flexible layer of material on the SiO_2 crystal.

4.2. Bacterial Viability

The bacterial viability was determined using a fluorescent live/dead assay. Images were collected for each trial, such as the image shown in Figure 9.
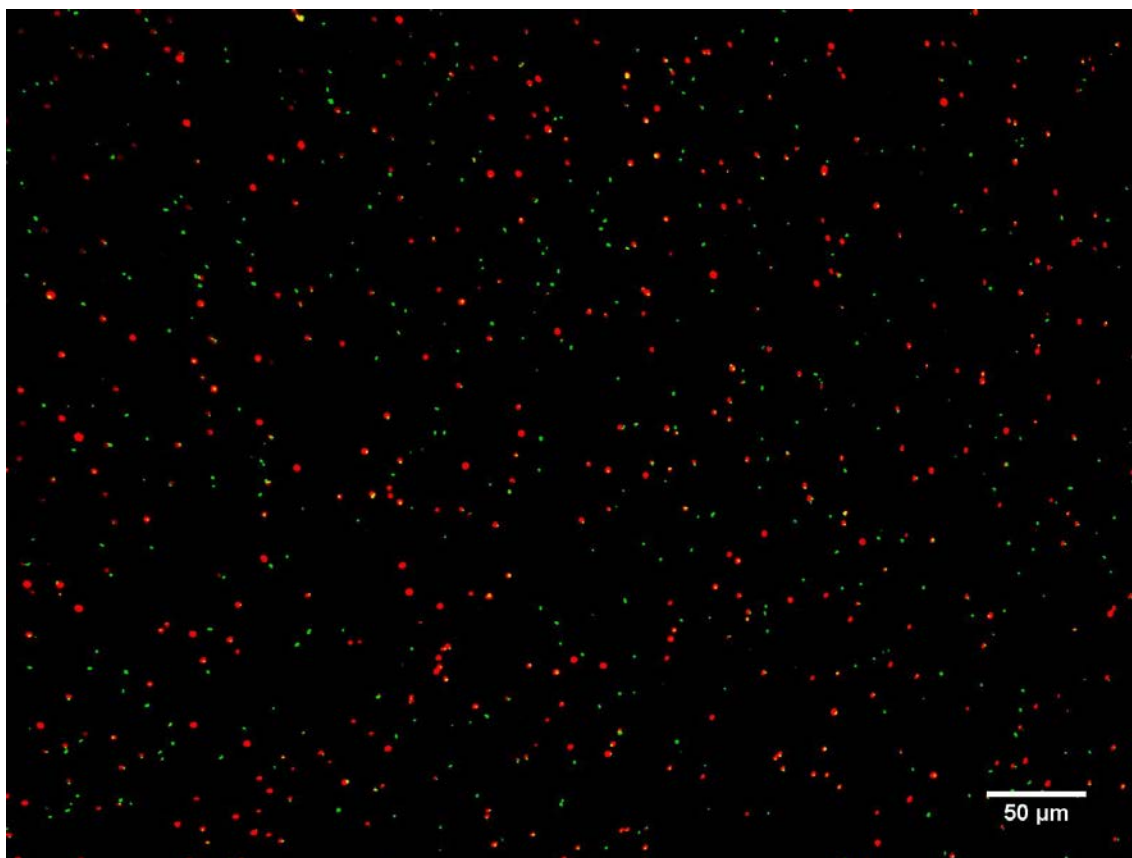
Figure 9. Image of *S. aureus* from live/dead bacterial viability assay.
Images were taken with a 20x objective using FITC and Texas Red filters. Image shown is a composite of the green and red images. Live cells (green) and dead cells (red) were counted separately in ImageJ. The percent of cells dead were calculated for each location on the crystal.

While examining each crystal, it was observed that the bacteria were not evenly distributed; some parts of the crystal had much higher densities of bacterial cells than others. Also, the killing percentage varied from location to location. To reduce the variation in later trials, images were taken of as many locations as possible per crystal before photobleaching was observed. An average of fifteen locations were imaged per crystal.

For the physically adsorbed peptide, the average killing percentage was 55% with a standard deviation of 14%. For the peptide covalently bound to the surface via a SM(PEG)$_{12}$ spacer molecule, the killing percentage was 39% with a standard deviation of 10%. These results indicate that the spacer molecule does have an effect on the ability of the immobilized peptide to

kill the bacteria. A summary of the data reflecting the peptide adsorption or binding and the

antibacterial activity of the peptide is shown in Table 1 below.

Table 1. Comparison of changes in frequency, mass, and percent dead cells for the physically adsorbed peptide and peptide bound via a linker.

	Physically adsorbed peptide	Peptide bound through SM(PEG)$_{12}$ linker
Δf (hz) of peptide adsorption	10.0	71.2
Mass of peptide adsorbed (ng)	25.3	180
Percent of dead cells (*S. aureus*)	55 ± 14	39 ± 10

5. Discussion

The prevalence of bacterial infections, particularly those resistant to traditional antibiotics, calls for a novel approach to preventing such infections. The ability to create antimicrobial surfaces could provide a potential solution to this problem, particularly for food processing or medical implant related infections. Antimicrobial peptides are an attractive candidate for this approach since bacteria are generally unable to develop resistance to AMPs. However, based on the proposed mechanisms of action of AMPs, the peptides may need more flexibility than direct immobilization allows in order to appropriately align and interact with bacteria to cause bacterial death. The use of a flexible spacer molecule could provide the advantages of a covalent attachment while maintaining the necessary freedom for AMP activity.

This study concluded that there was an increase in peptide adsorption to the surface when the peptide was attached with a flexible spacer molecule compared to the peptide being physically adsorbed to the surface. The data shows that peptide bound with a spacer molecule had a decreased percentage of dead bacteria on the surface compared to the peptide that was physically adsorbed to the surface. Data from this study showed that there may be a correlation between the mass of the peptide adsorbed to the surface and the ability of the peptide to kill the bacteria (Figure 10), which is consistent with what has been reported in the literature (Bagheri, Beyermann and Dathe 2009, Chen, et al. 2009, Appendini and Hotchkiss 2001). Since the killing percentage did not increase proportionally with the amount of peptide on the surface, there may be additional factors affecting the ability of the peptide to effectively kill bacteria.
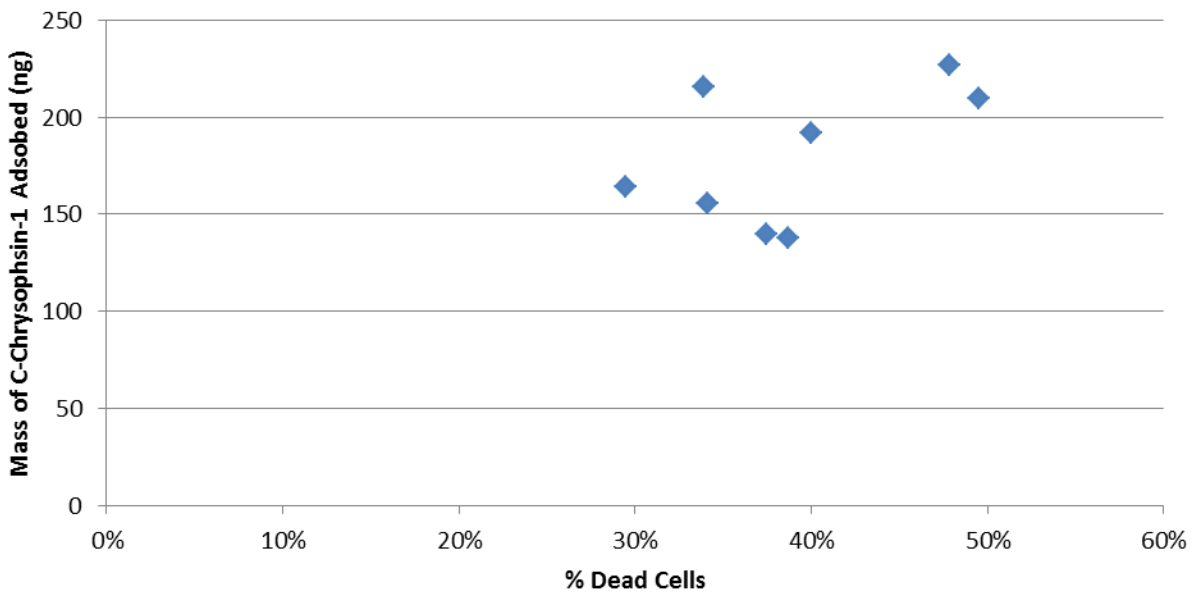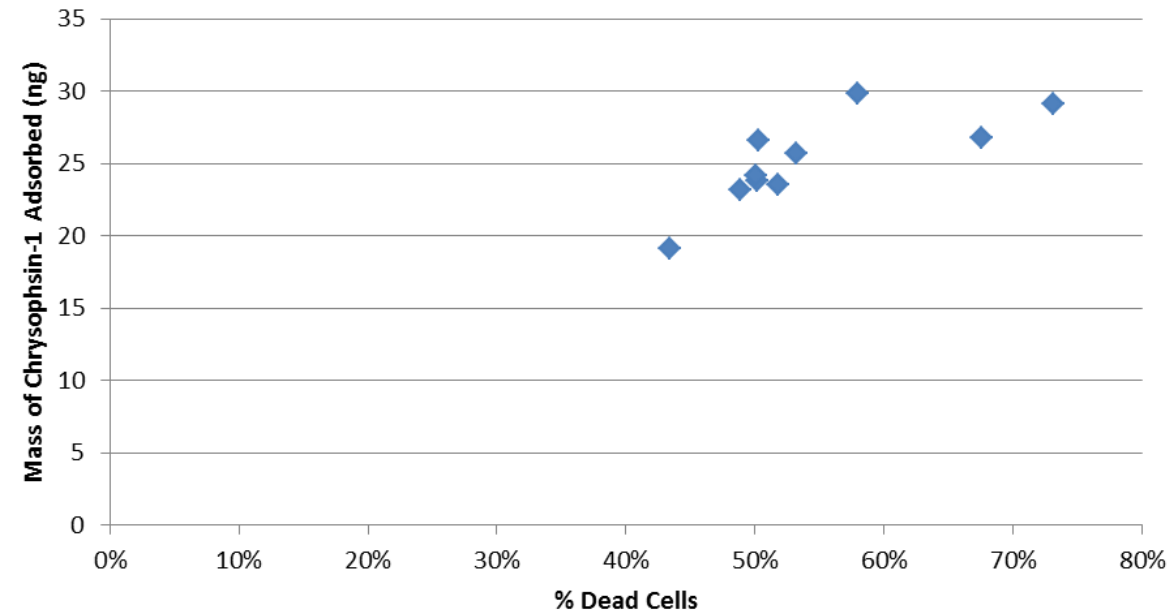
Figure 10. Comparison of the killing percentage to the amount of Chrysophsin-1 physically adsorbed to the surface (top) or C-Chrysophsin-1 bound to the surface via a SM(PEG)$_{12}$ spacer (bottom).
The mass of peptide bound to the surface was calculated using the change in frequency and the Sauerbrey Equation (equation 1). There appears to be a general trend indicating that more peptide present on the surface correlates with improved antibacterial property of the surface.

In previous studies, chrysophsin-1 was found to effectively kill gram-negative bacteria when attached to a surface with SM(PEG)$_{12}$ (Ivanov, et al. 2012). A killing percentage of 80-90% was previously observed when using *E. coli*. However, S. *aureus* in particular has been shown to be less responsive to immobilized antimicrobial peptides than other gram-positive bacteria, though the reason for this difference is unclear (Appendini and Hotchkiss 2001). One possible hypothesis to explain the decreased killing percentage for both the physically adsorbed peptide and the covalently bound chrysophsin-1 with gram-positive bacteria could be the difference in the cell wall structure of gram-positive bacteria. Differences in cell wall and cell membrane structure affect the conformation in which the peptide must be to effectively interact with the cell (Sani, Whitwell and Separovic 2012). Therefore, the thick peptidoglycan layer may not allow the peptide to interact with the bacterial cell membrane in such a way that the AMP can effectively cause cell death.

The differences in cell wall structure may require the peptide to be attached to the surface with a different length spacer molecule to effectively kill gram-positive bacteria. Previous studies have suggested that longer spacer molecules can help to improve antibacterial properties of immobilized AMPs. It is speculated that shorter spacer lengths may not allow the peptide to interact with and permeate the membrane (Bagheri, Beyermann and Dathe 2009). Therefore, a longer spacer molecule may improve the killing percentage of *S. aureus* by C-CHY1 when immobilized.

The decreased killing percentage could also be due to the concentration of the AMP on the surface; the concentration of peptide present may not be sufficient to achieve the 80-90% killing that has been previously observed (Ivanov, et al. 2012). Peptide concentration has been shown to be an important factor in antimicrobial activity (Onaizi and Leong 2011). The

uniformity or level of saturation of the peptide on the surface was not characterized. The variation in both cell coverage and killing percentage observed between different locations on each crystal is likely due to the crystal surface not being uniformly covered with peptide (Figure 11). Future work could include further characterizing the density and uniformity of the peptide adsorption on the crystal surface and investigating potential correlations between amount of peptide on the surface and the antimicrobial efficacy of the peptide.
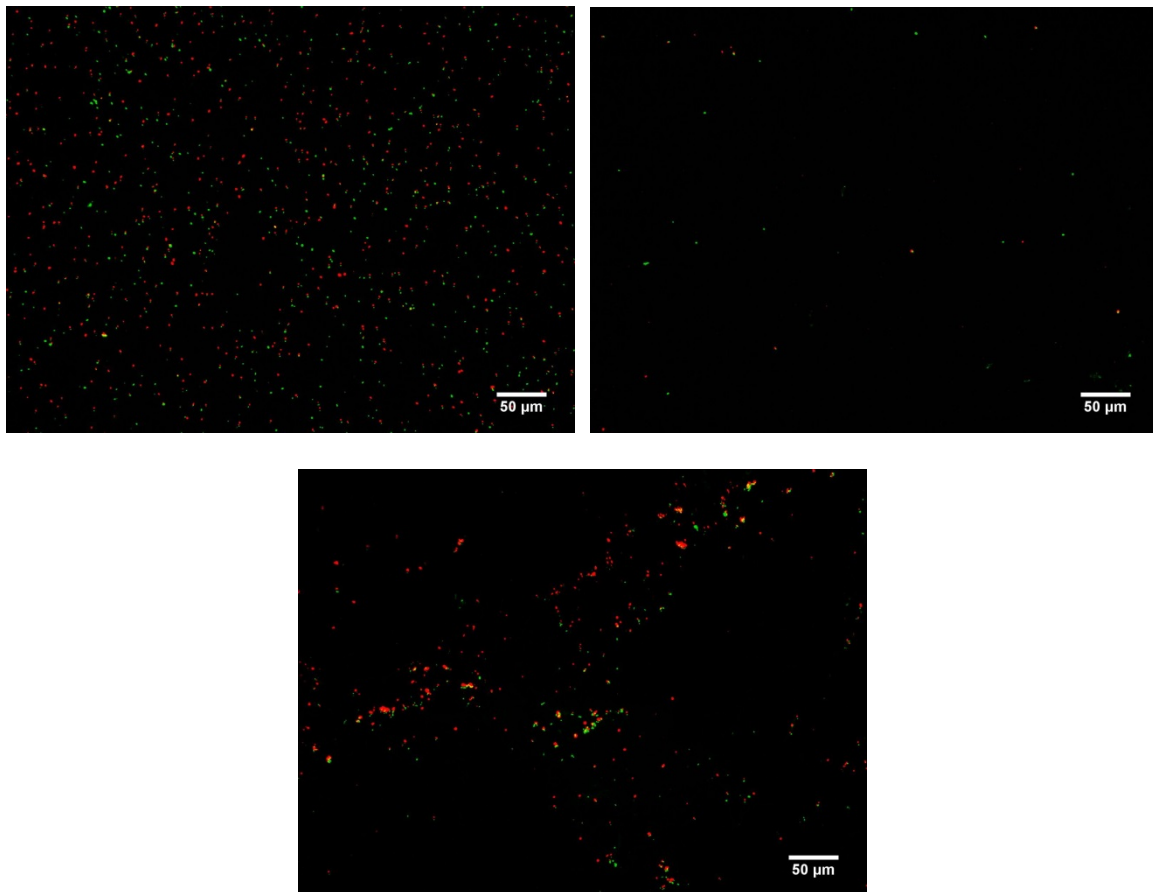
Figure 11. Example images demonstrating variability in density of cells.
Composite images from various locations on the same crystal. Some locations showed a consistent high density of cells, other locations show very few cells, and other locations showed an uneven distribution of cells on the surface.

One additional factor may have been the potential degradation of the peptide. The unmodified CHY1 was diluted, aliquoted, and frozen, while the stock solution of C-CHY1 was thawed for each experiment. As more freeze/thaw cycles occurred, more variability was

observed, suggesting that this process could be affecting the peptide. The repeated freeze/thaw cycles may have had an effect on the efficacy of the peptide, in terms of both peptide binding to the linker molecule and the antibacterial activity of the peptide.

The Sauerbrey Equation, which was used to calculate the mass of the adsorbed peptide and bacteria, is also a potential source of error in this experiment. The Sauerbrey Equation is most accurate when considering very rigid films on the surface of a crystal because less rigid films will not fully couple the oscillations of the viscoelastic layer to the crystal. As the layer on the crystal becomes less rigid, the Sauerbrey Equation will underestimate the mass being added to the crystal. Therefore, the mass adsorbed to the surface during the peptide adsorption may be higher than calculated. The significant increase in dissipation throughout the experiment suggested that frequency changes due to bacterial adsorption would not provide reasonable or accurate estimations of the mass adsorbed during this step. Therefore, changes in mass due to bacterial adsorption were not calculated. However, the Sauerbrey equation provides a reasonable approximation of the peptide adsorbed to the surface.

Some variability was observed between trials in the consistency of frequency changes between overtones. Some trials show each overtone with similar frequency changes, while other replicates, there were significant differences in overtones (Figure 12). This may have affected the average frequency changes calculated and thus the calculated mass adsorbed to the surface during the given step. The cause of this variability is unknown, since variability was observed even between replicates carried out simultaneously using all of the same materials and solutions.
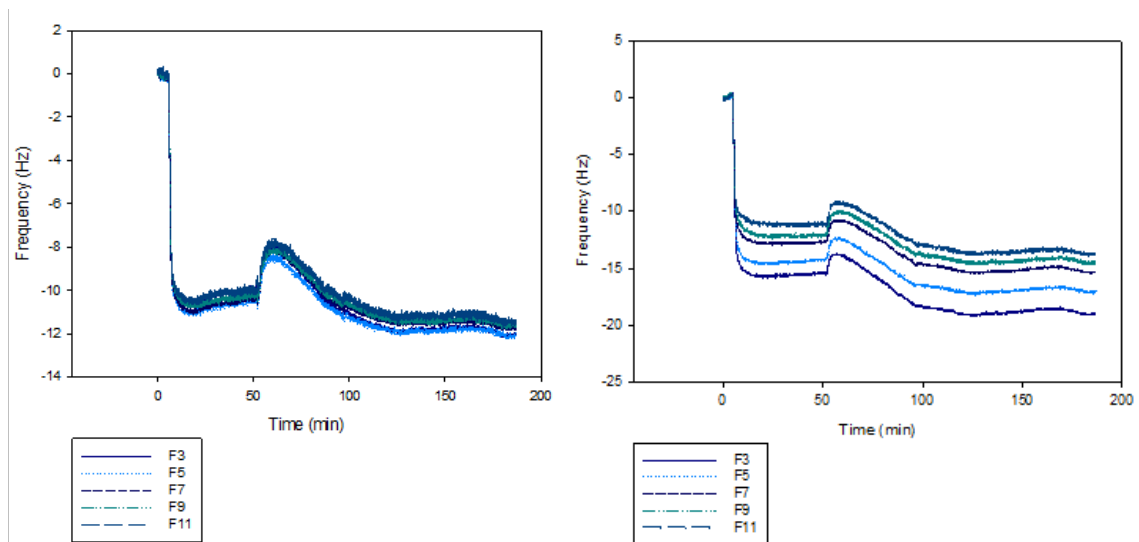
Figure 12. Frequency changes for physically adsorbed CHY1.
Frequency changes for physically adsorbed CHY1 replicates carried out simultaneously in . This demonstrates the variability observed in overtones and frequency change between replicates.

6. Conclusions and Recommendations

The effect of immobilizing chrysophsin-1 via a covalent attachment to a flexible SM(PEG)$_{12}$ linker molecule was studied. This immobilization approach decreased the ability of the peptide to kill *S. aureus* when compared to peptide that was physically adsorbed to the surface. However, a different length of linker molecule may allow the peptide more freedom to interact with and potentially permeate the thick peptidoglycan layer of the gram-positive bacteria. Therefore, additional linker molecule lengths should be studied to determine if a linker molecule of a different length could allow the peptide to more effectively kill gram-positive bacteria.

Data suggests that the surface of the crystal may not be saturated when the peptide was bound via a linker molecule (Figure 7 and Figure 11). Increasing the amount of peptide bound to the surface may improve the antibacterial properties of the immobilized peptide. Also, the density and uniformity of the peptide bound to the surface should be characterized in order to determine if this has an effect on the efficacy of the peptide. The effect of repeated freezing and thawing of the peptide should be studied to determine the effect that this process has on the ability of the peptide to bind to the SM(PEG)$_{12}$ linker, as well as its ability to disrupt the cell membranes of the *S. aureus* bacteria.

Additionally, previous studies had manually counted the number of live and dead cells on the crystal surface, while images from this study were counted using ImageJ software (Ivanov, et al. 2012). This may have had an effect on the calculated killing percentages since there may have been inconsistencies in exactly what was counted as a cell. The experiments with gram-negative bacteria should be repeated and the images analyzed with ImageJ software to determine if the counting procedure had any effect on the calculated killing percentage.

There was a significantly higher mass of peptide present when the C-CHY1 was bound to the surface via a linker molecule, so it was expected that the killing percentage would have been much higher than when the peptide was physically adsorbed onto the surface. Since the killing percentage for the $(SM)PEG_{12}$/C-CHY1 system did not increase proportionally with the increase in mass compared to the physically adsorbed peptide, the binding of the C-CHY1 to the surface via the linker molecule may be inhibiting the ability of the peptide to disrupt the bacterial membrane. However, the peptide will likely remain on the surface longer when it is covalently attached compared to when it is physically adsorbed. Therefore, for practical applications, one may need to compromise killing percentage for durability of the antimicrobial surface. The use of a spacer molecule for attaching AMPs to a surface shows promise for various applications, however parameters such as concentration and spacer length should be optimized.

References

Appendini, P., and J. H. Hotchkiss. "Surface Modification of Poly(styrene) by the Attachment of an Antimicrobial Peptide." *Journal of Applied Polymer Science* 81 (2001): 609-616.

Arcidiacono, Steven, Philip Pivarnik, Charlene M. Mello, and Andre Senecal. "Cy5 labeled antimicrobial peptides for enhanced detection of Escherichia coli O157:H7." *Biosensors and Bioelectronics* 23 (2008): 1721-1727.

Bagheri, Mojtaba, Michael Beyermann, and Margitta Dathe. "Immobilization Reduces the Activity of Surface-Bound Cationic Antimicrobial Peptides with No Influence upon the Activity Spectrum." *Antimicrobial Agents and Chemotherapy* 53, no. 3 (2009): 1132-1141.

Baron, S. *Medicinal Microbiology.* Galveston, 1996.

Berney, Michael, Frederik Hammes, Franziska Bosshard, Hans-Ulrich Weilenmann, and Thomas Egli. "Assessment and Interpretation of Bacterial Viability by Using the LIVE/DEAD BacLight Kit in Combination with Flow Cytometry." *Applied and Environmental Microbiology* 73, no. 10 (May 2007): 3283-3290.

Brana, Corrine, Chris Benham, and Lars Sundstrom. "A method for characterising cell death in vitro by combining propidium iodide staining wiht immunohistochemistry." *Brain Research Protocols* 10 (2002): 109-114.

Brogden, K A. "Antimicrobial peptides: pore formers or metabolic inhibitors?" *Nature Reviews Microbiology*, 2005: 238-250.

CDC 2011 Estimates: Findings. February 2012. http://www.cdc.gov/foodborneburdan/2011-
foodborne-estimates.html.

Chen, Renxum, et al. "Synthesis, characterization and in vitro activity of a surface-attached
antimicrobial cationic peptide." *Biofouling* 25 (2009): 517-524.

Costa, Fabiola, Isabel F. Carvalho, Ronald C. Montelaro, P. Gomes, and M. Cristina L. Martins.
"Covalent immobilization of antimicrobial peptides (AMPs) onto biomaterial surfaces."
Acta Biomaterialia 7 (2011): 1431-1440.

Cronin, C, and A Kadilak. *Utilizing the Quartz Crystal Microbalance with Dissipation to bind
cecropin P1 to Escherichia coli.* Worcester: Worcester Polytechnic Institute Department
of Chemical Engineering, Chemistry, and Biochemisty, 2008.

Elwing, Hans, Malte Hermansson, and Karen Otto. "Effect of Ionic Strength on Initial
Interactions of Escherichia coli with Surfaces, Studied on-line by a Novel Quartz Crystal
Microbalance Technique." *Journal of Bacteriology* (American Society for Microbiology)
181, no. 17 (September 1999): 5210-5218.

Glinel, Karine, Alain M. Jonas, Thierry Jouenne, Jerome Leprince, Ludovic Galas, and Wilhelm
T. S. Huck. "Antibacterial and Antifouling Polymer Brushes Incorporating Antimicrobial
Peptide." *Bioconjugate Chemistry* 20 (2009): 71-77.

Gregory, Kalvin, and Charlene M. Mello. "Immobilizaiton of Escherichia coli Cells by Use of
the Antimicrobial Peptide Cecropin P1." *Applied and Environmental Microbiology* 71,
no. 3 (2005): 1130-1134.

Haynie, Sharon L., Grace A. Crum, and Bruce A. Doele. "Animicrobial Activities of

    Amphiphilic Peptides Covalently Bonded to a Water-Insoluble Resin." *Antimicrobial*

    Agents and Chemotherapy 39, no. 2 (1995): 301-307.

Ivanov, Ivan E., Alec E. Morrison, Jesse E. Cobb, Catherine A. Fahey, and Terri A. Camesano.

    "Creating Antibacterial Surfaces with the Peptide Chrysophsin-1." *ACS Applied*

    Materials and Interfaces, no. 4 (October 2012): 5891-5897.

Kulagina, Nadezhda V., Michael E. Lassman, Frances S. Ligler, and Chris Rowe Taitt.

    "Antimicrobial Peptides for Detection of Bacteria in Biosensor Assays." *The Journal of*

    Analytical Chemistry 77 (2005): 6504-6508.

Molecular Probes. *Propidium Iodide Nucleic Acid Stain.* Invitrogen, 2006.

Molecular Probes. *SYTO(R) Green-Fluorescent Nucleic Acid Stains.* Invitrogen, 2011.

Onaizi, Sagheer A., and Susanna S. J. Leong. "Tethering antimicrobial peptides: Current status

    and potential challenges." *Biotechnology Advances* 29 (2011): 67-74.

Q-Sense, Inc. "Quartz Crystal Microbalance with Dissipation (QCM-D)." *Technology Note.* n.d.

    http://www.q-sense.com/file/qcm-d-technology-note.pdf (accessed 2012 йил 26-

    September).

Sani, Marc-Antoine, Thomas C. Whitwell, and Frances Separovic. "Lipid composition regulates

    the conformation and insertion of the antimicrobial peptide maculatin 1.1." *Biochimica et*

    Biophysica Acta 1818 (2012): 205-211.

Strauss, J, A Kadilak, C Cronin, C M Mello, and T A Camesano. "Binding, inactivation, and

    adhesion forces between antimicrobial peptide cecropin P1 and pathogenic E. coli."

    Colloids and Surfaces B: Biointerfaces 75 (2010): 156-164.

Uzarski, Joshua R., Alba Tannous, John R. Morris, and Charlene M. Mello. "The effects of

    solution structure on the surface conformation and orientation of a cysteine-terminated

    antimicrobial peptide cecropin P1." *Colloids and Surfaces B: Biointerfaces* 67 (2008):

    157-165.

Wang, Kathleen F., Ramanathan Nagarajan, Charlene M. Mello, and Terri A. Camesano.

    "Characterization of Supported Lipid Bilayer Disruption By Chrysophsin-3 Using QCM-

    D." *The Journal of Physical Chemistry B* (American Chemical Society), no. 115 (2011):

    15228-15235.

Westphal, D, G Dewson, P E Czabotar, and R M Kluck. "Molecular Biology of Bax and Bak

    activation and action." *Biochimica et Biophysica Acta (BBA)-Molecular Cell Research*

    1813 (2011): 521-531.

Appendix A: *S. aureus* **Growth Curve**

S. aureus Growth Curve
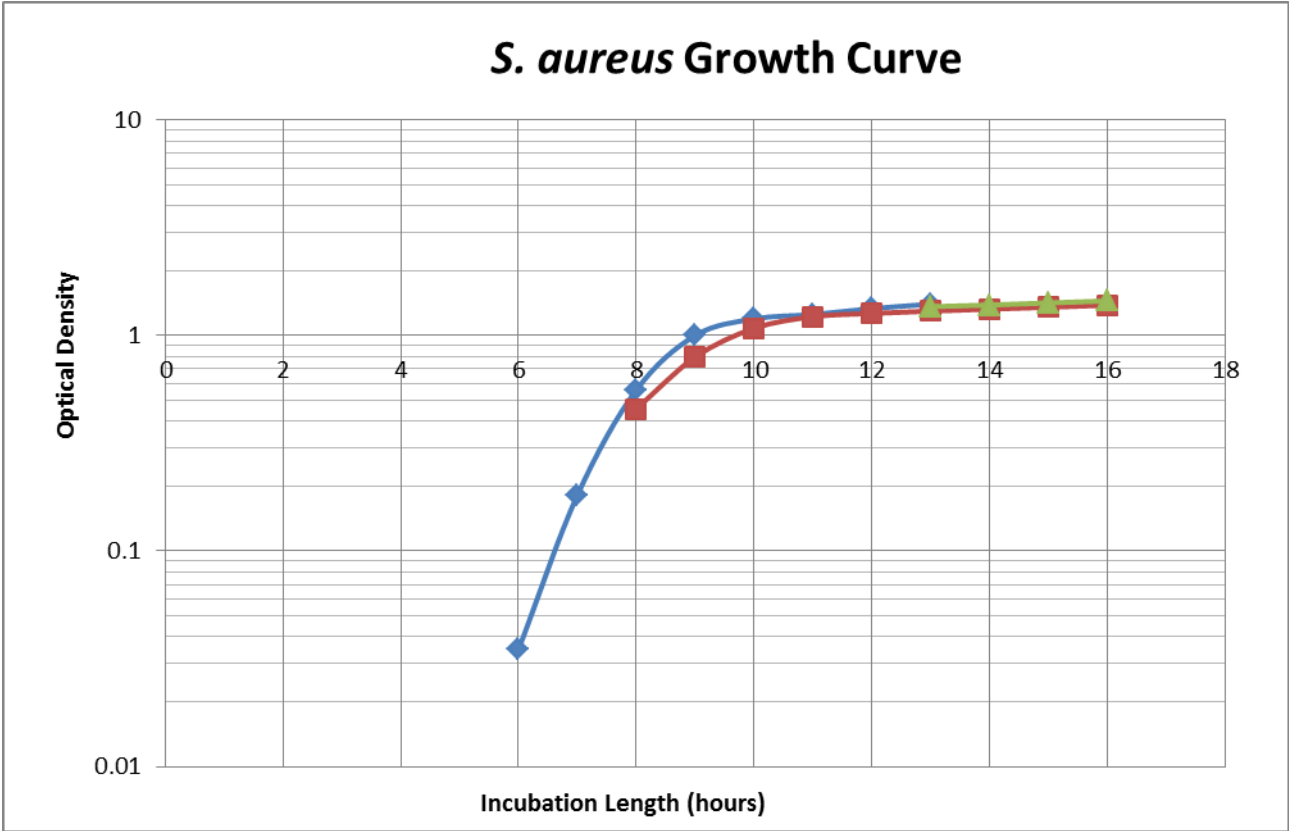
Appendix B: QCM-D Frequency and Dissipation Plots

Physically Adsorbed Chrysophsin-1

Control Trial 5 Chamber 1

Control Trial 5 Chamber 1

Control Trial 5 Chamber 2

Legend:
- F3
- F5
- F7
- F9
- F11

Control Trial 5 Chamber 2

Legend:
- F3
- F5
- F7
- F9
- F11
- D3
- D5
- D7
- D9
- D11

Control Trial 5 Chamber 3

Control Trial 5 Chamber 3

41
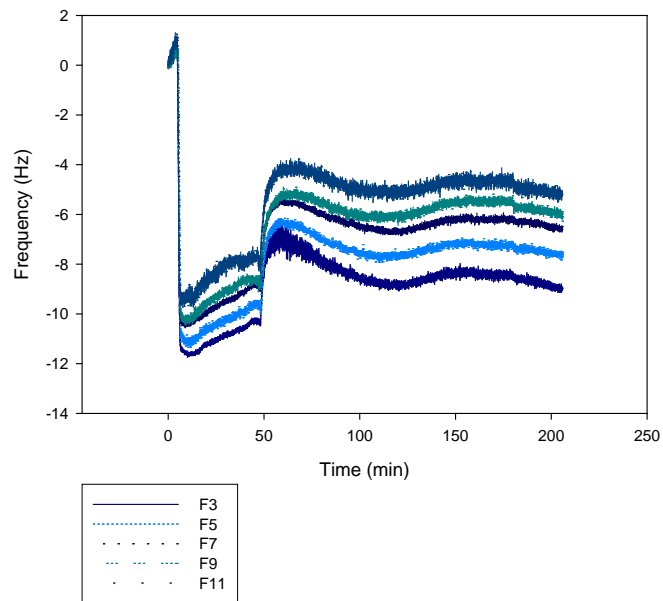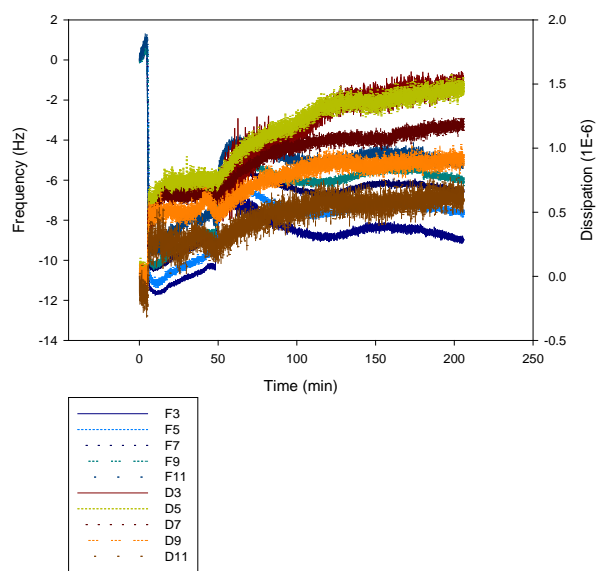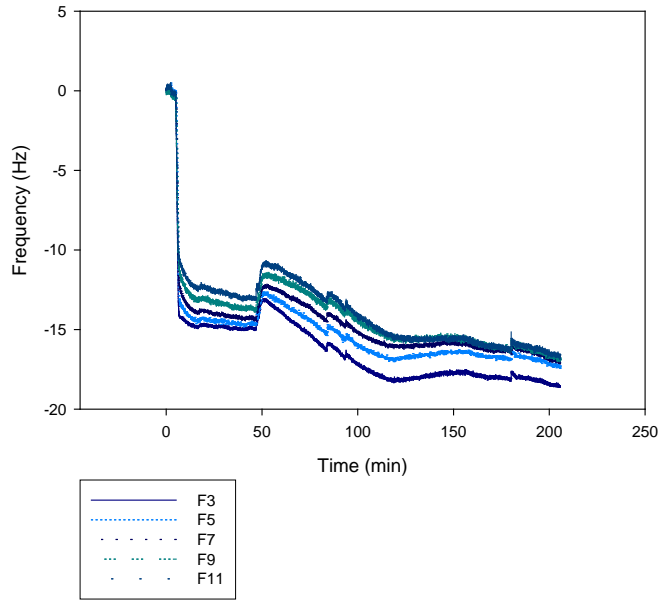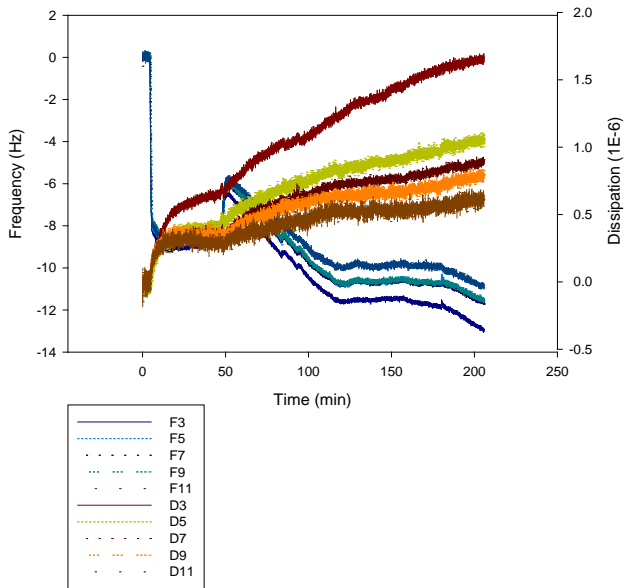
Control Trial 6 Chamber 2

Control Trial 6 Chamber 2
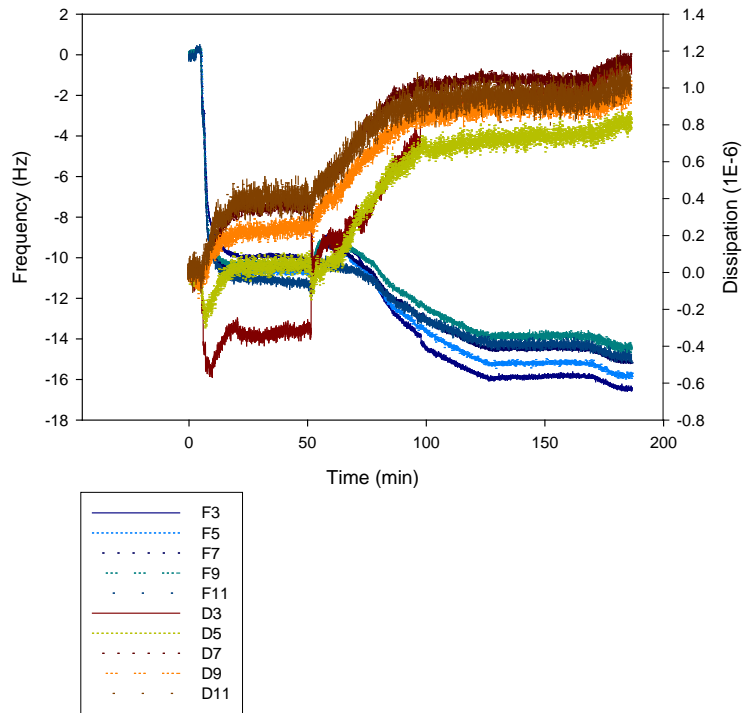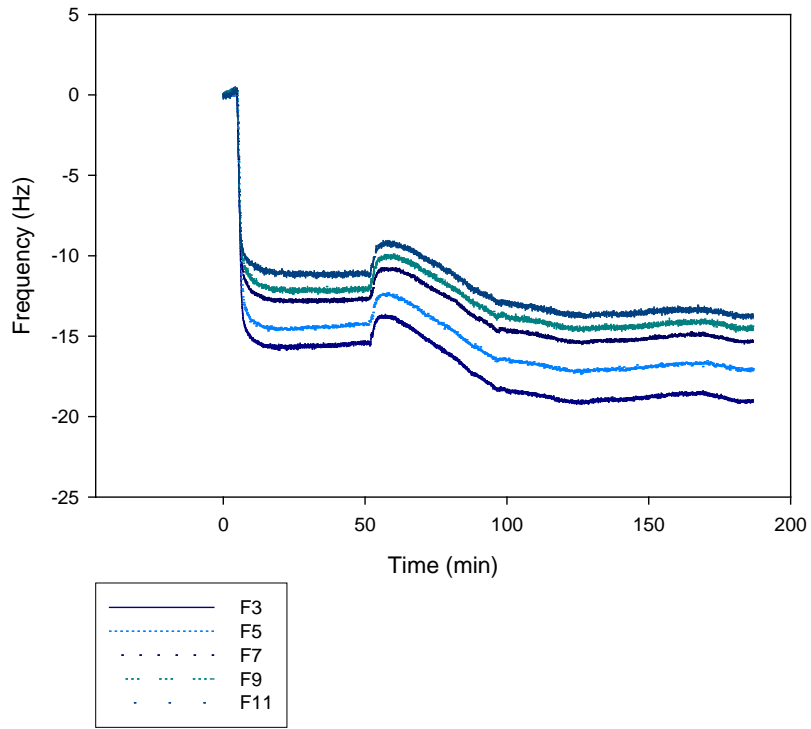
42

Control Trial 6 Chamber 3

Control Trial 6 Chamber 3
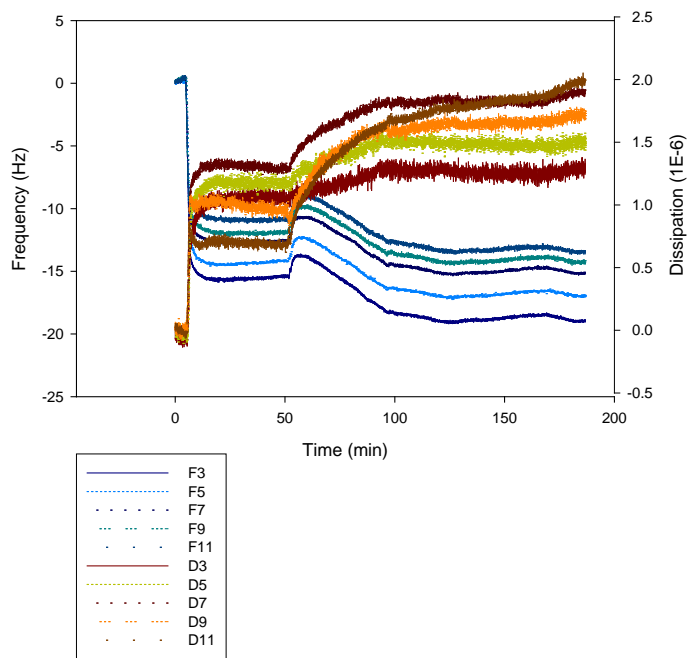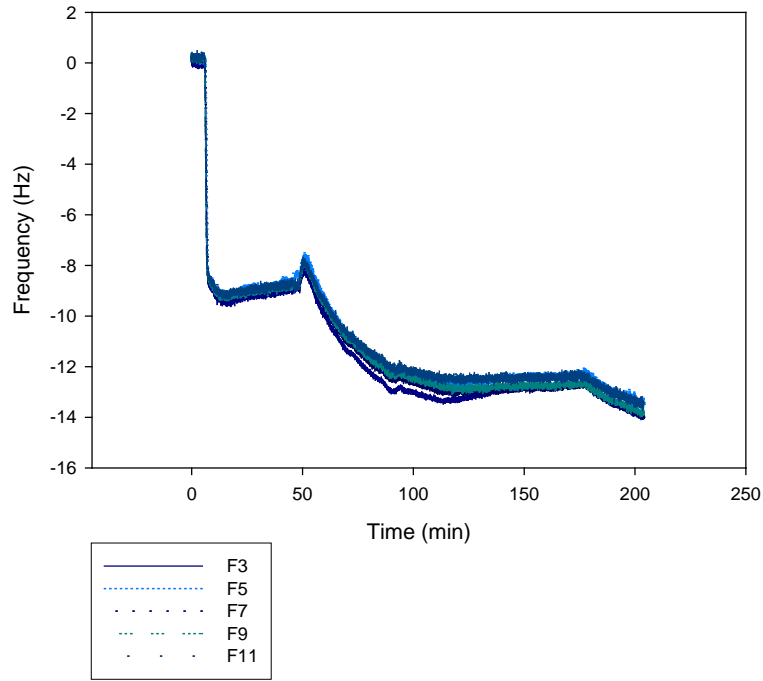
Control Trial 7 Chamber 1

Legend:
- F3
- F5
- F7
- F9
- F11

Control Trial 7 Chamber 1

Legend:
- F3
- F5
- F7
- F9
- F11
- D3
- D5
- D7
- D9
- D11
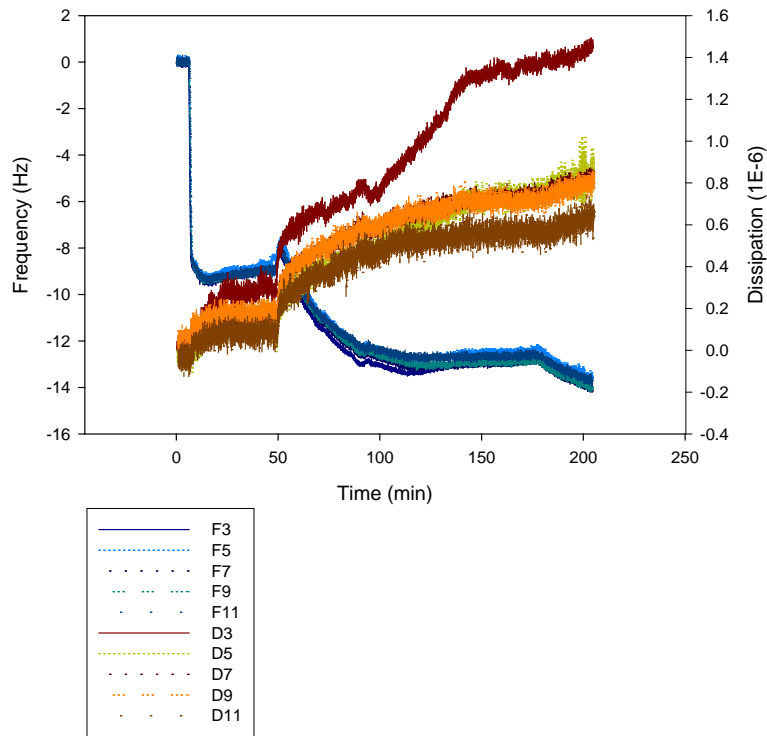
Control Trial 7 Chamber 3
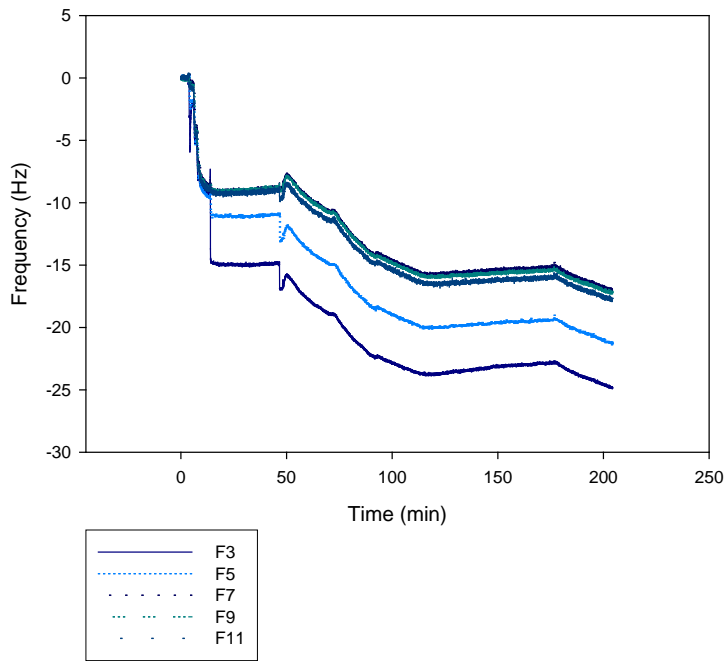
Control Trial 7 Chamber 3
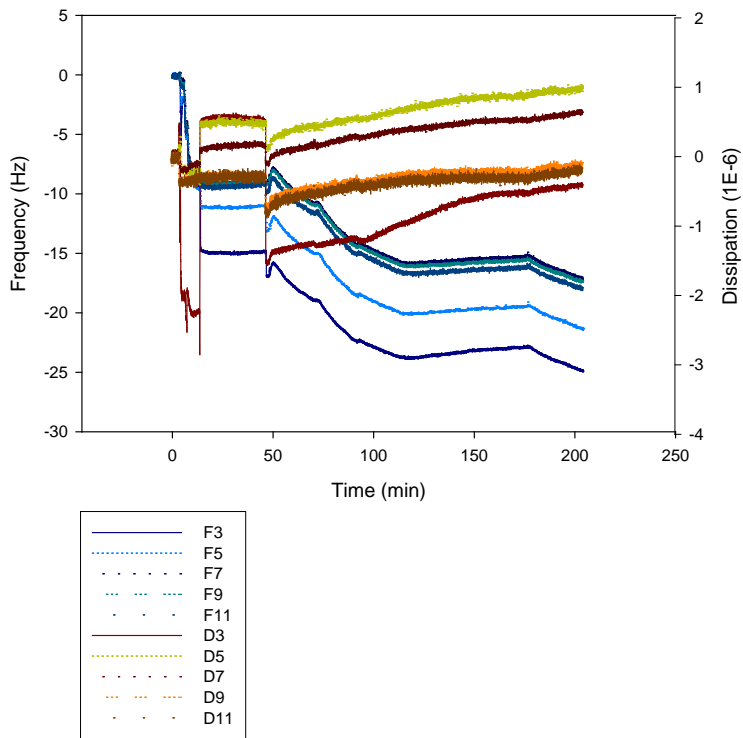
Control Trial 7 Chamber 4
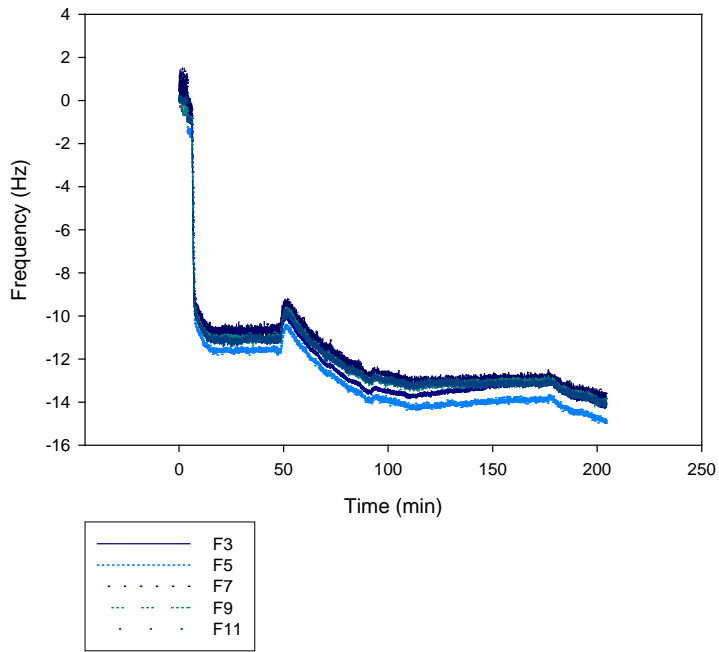
Control Trial 7 Chamber 4
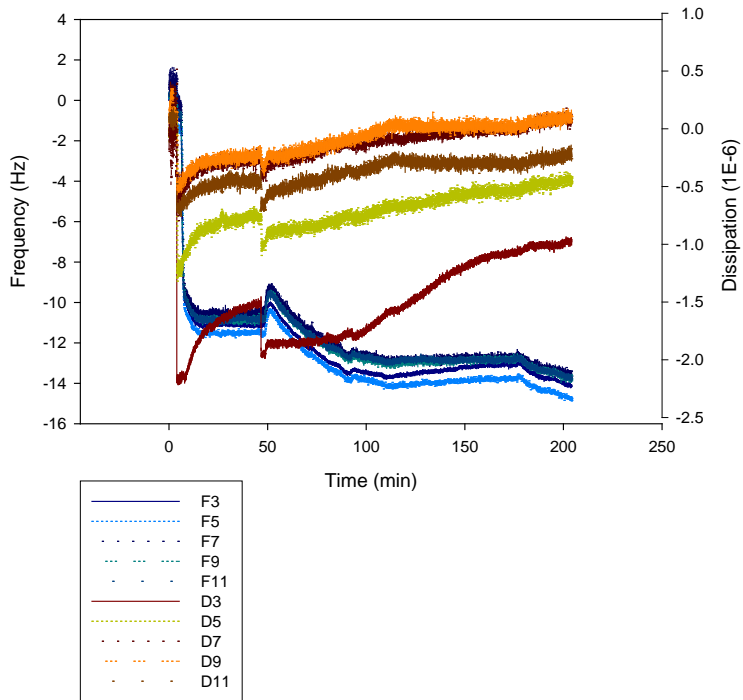
Trial 10 Chamber 2
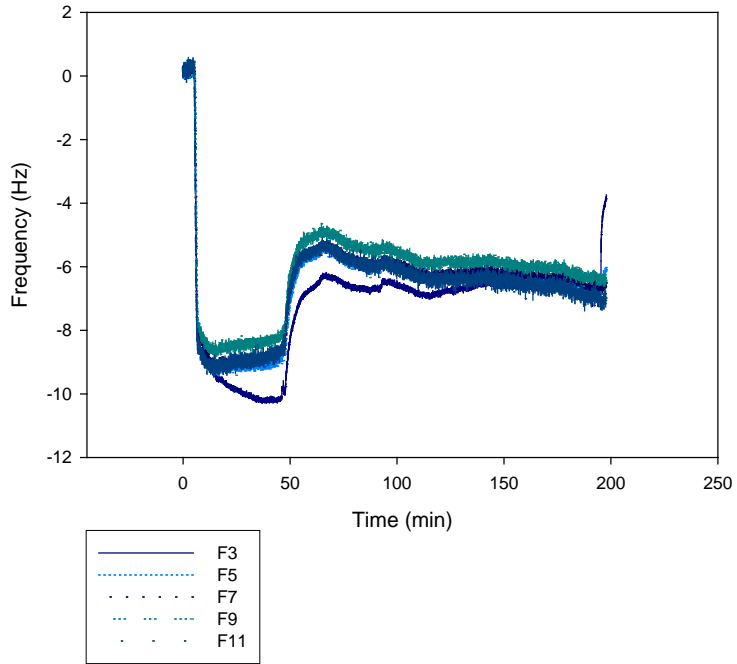
Trial 10 Chamber 2
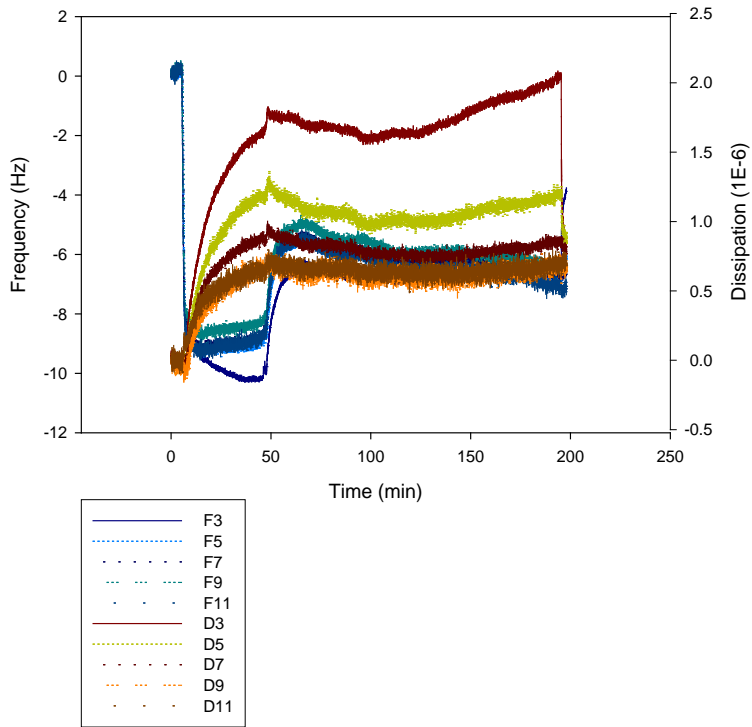
Trial 10 Chamber 4

Trial 10 Chamber 4

48
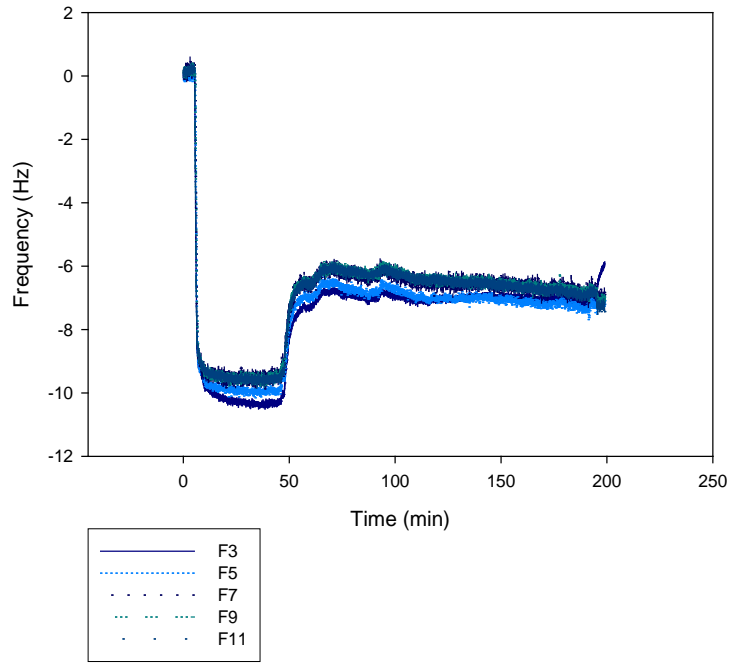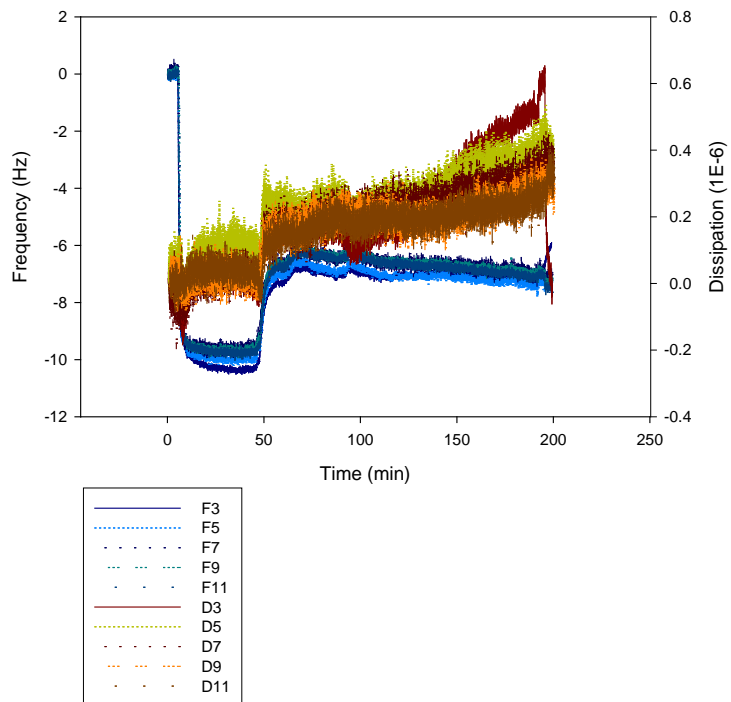
C-chrysophsin-1 Bound via an SM(PEG)₁₂ Linker

Full Procedure Trial 1 - Chamber 1
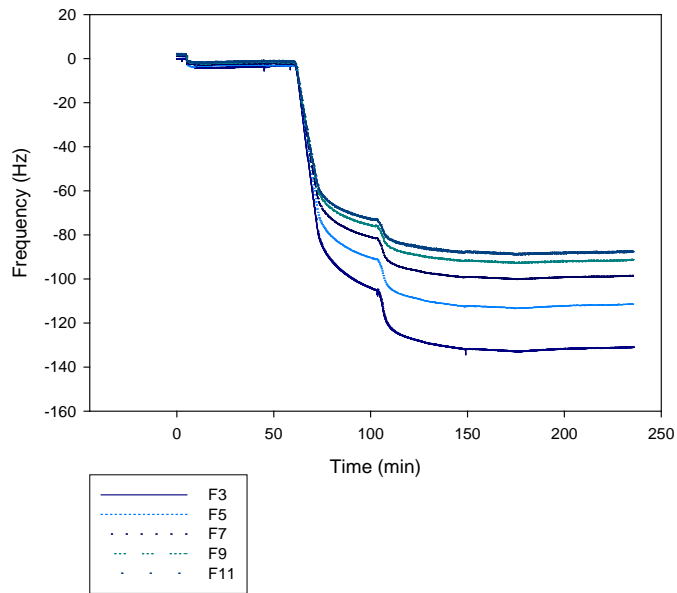
Full Procedure Trial 1 Chamber 1
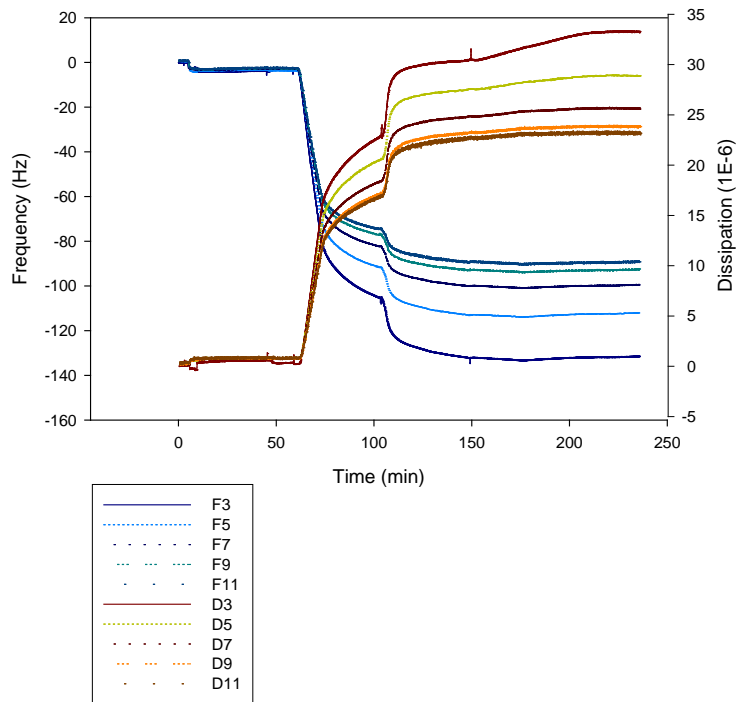
Full Procedure Trial 1 - Chamber 2
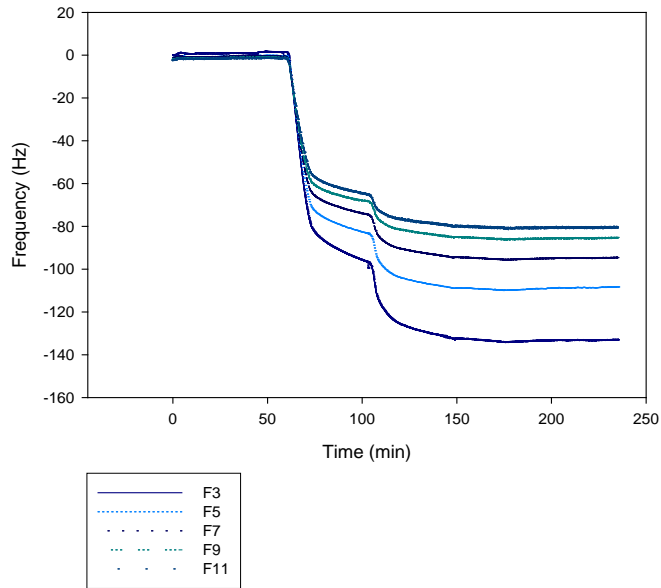
Full Prodedure Trial 1 Chamber 2
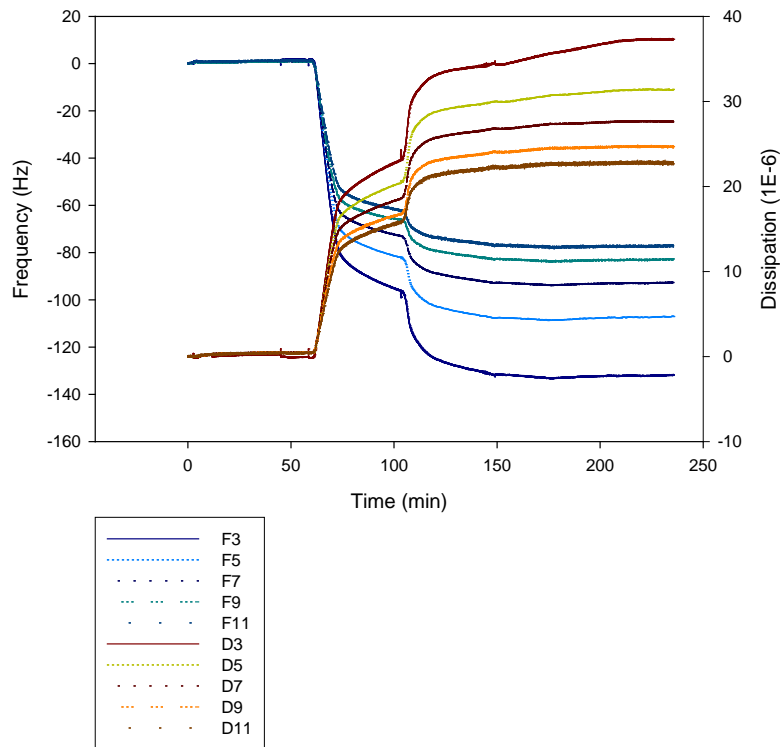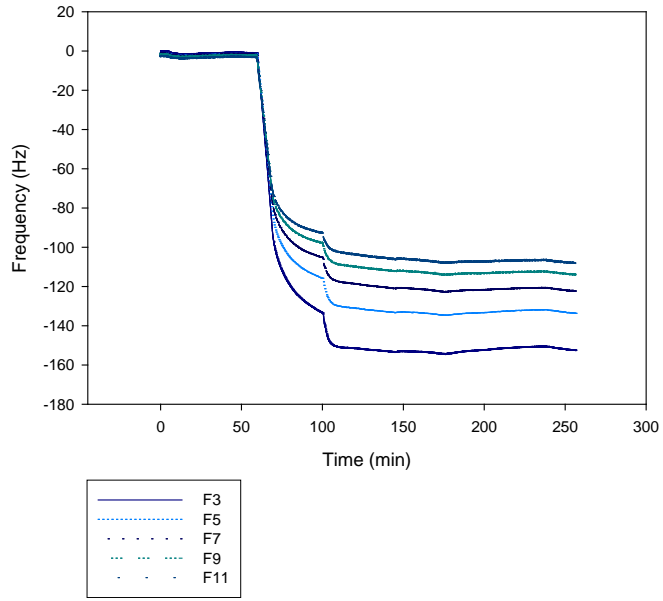
Full Procedure Trial 2 - Chamber 1

Full Procedure Trial 2 - Chamber 1

51
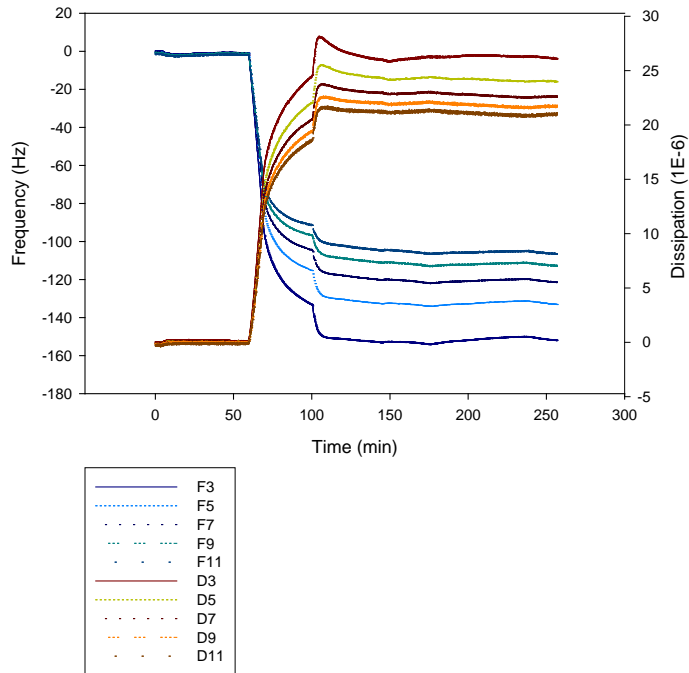
Full Procedure Trial 2 - Chamber 2
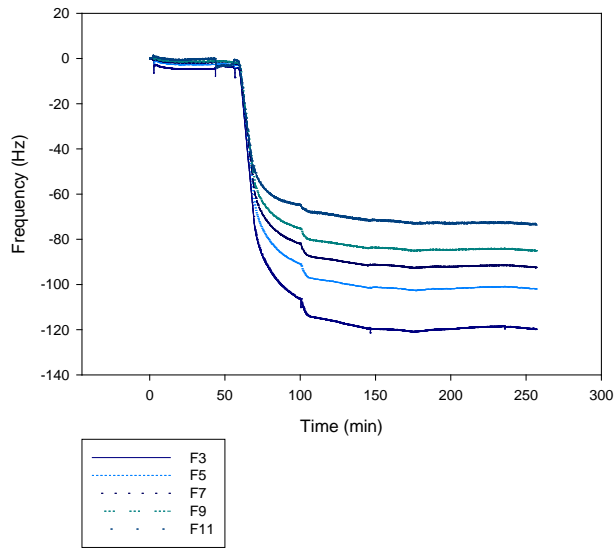
Full Procedure Trial 2 - Chamber 2
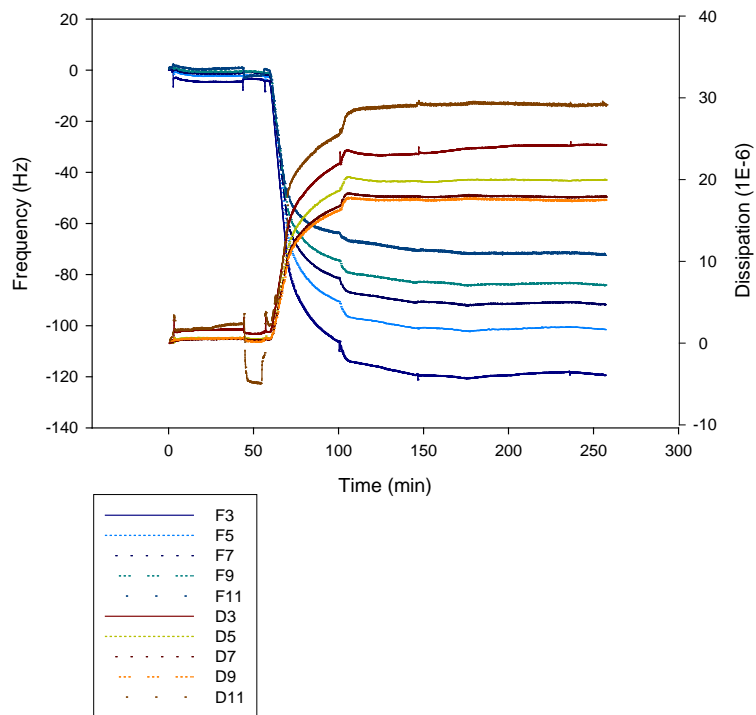
SM(PEG)$_{12}$ Trial 5 Chamber 1
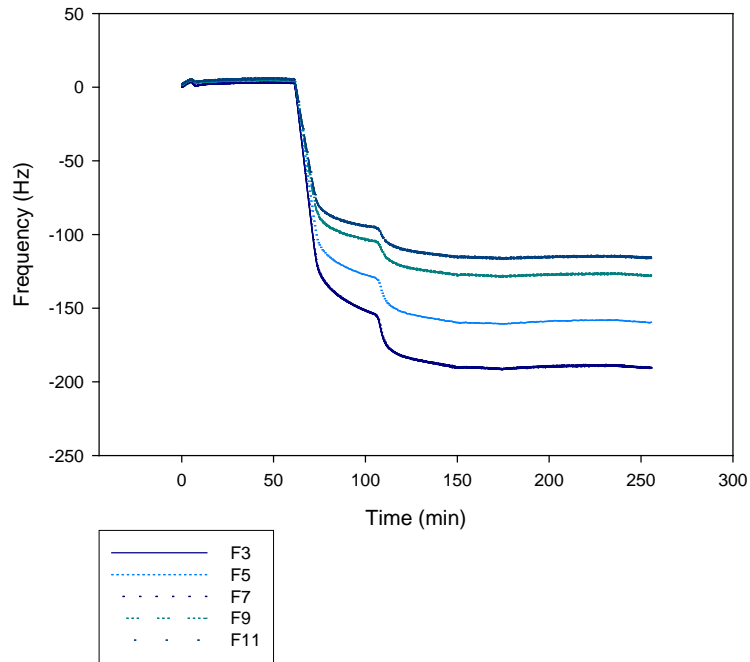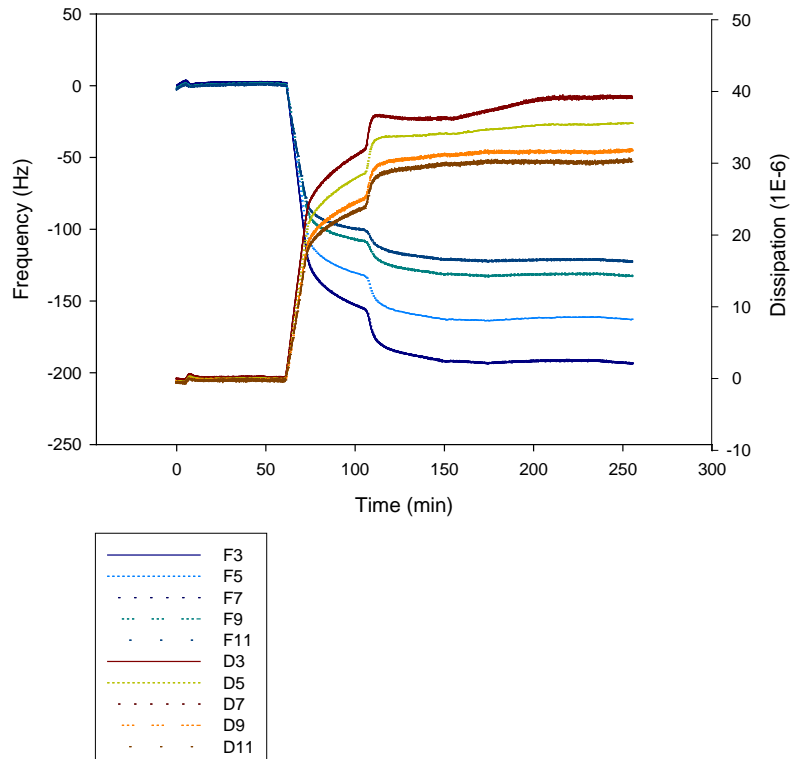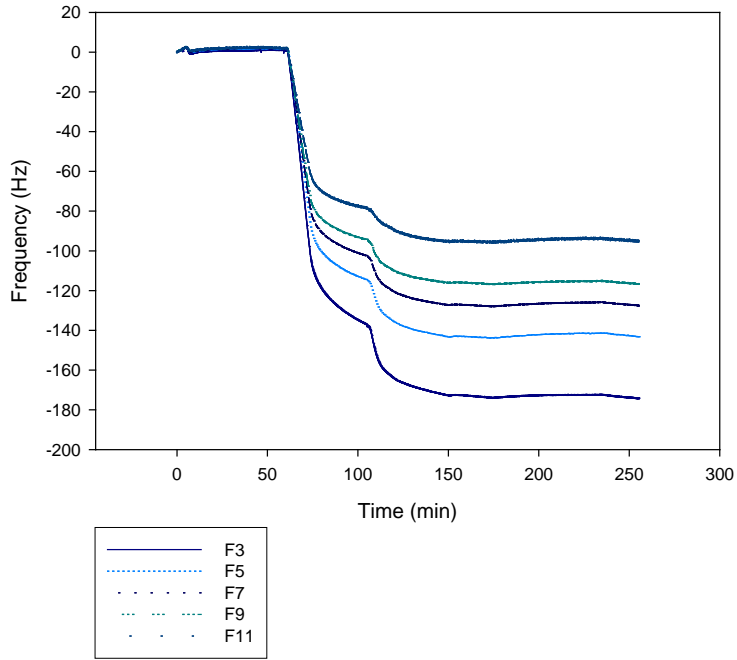
SM(PEG)$_{12}$ Trial 5 Chamber 1

SM(PEG)$_{12}$ Trial 5 Chamber 2

SM(PEG)$_{12}$ Trial 5 Chamber 2
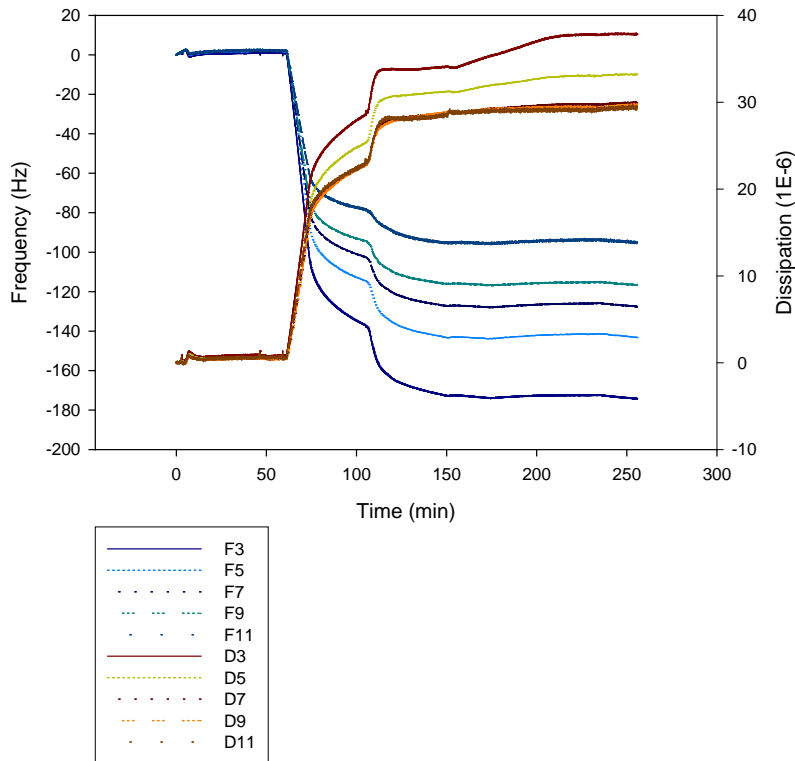
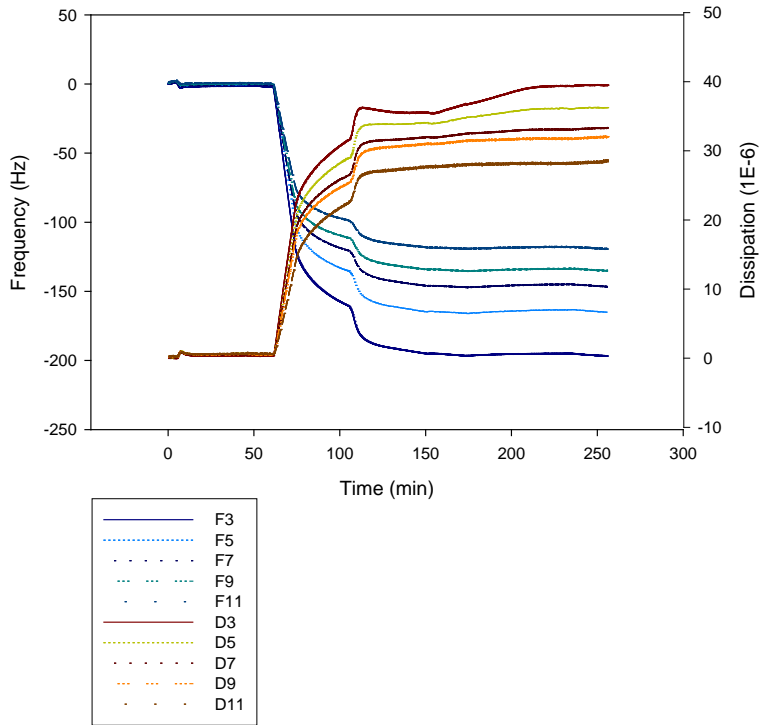SM(PEG)$_{12}$ Trial 5 Chamber 3
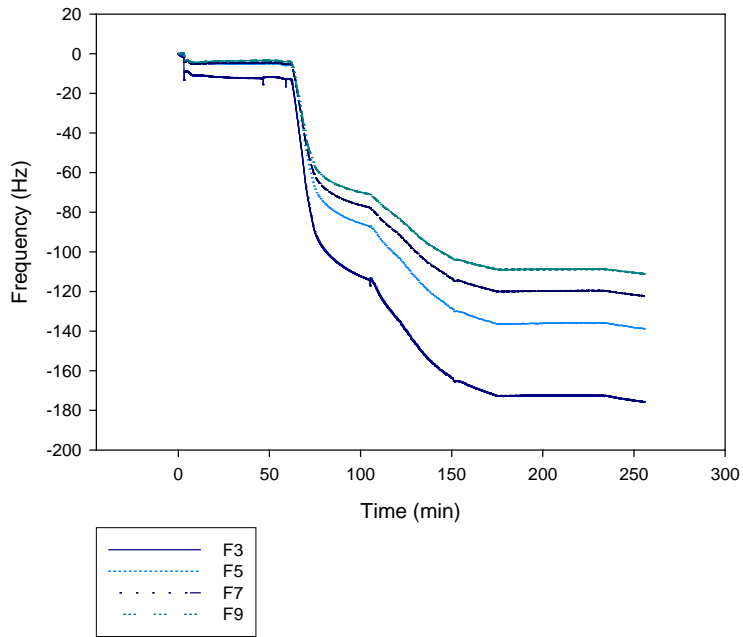
SM(PEG)$_{12}$ Trial 5 Chamber 3
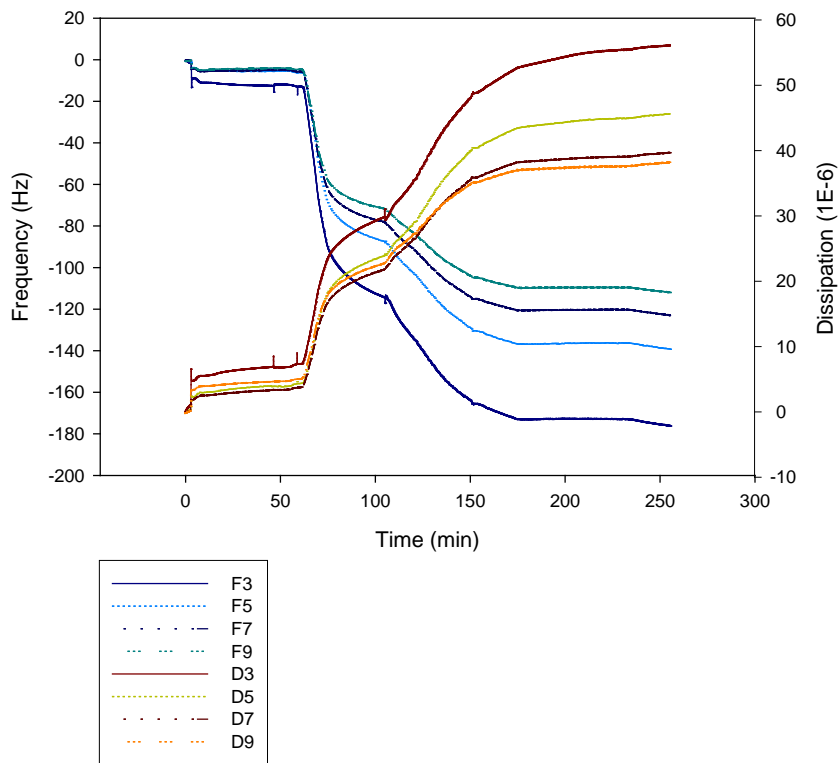
SM(PEG)$_{12}$ Trial 5 Chamber 4
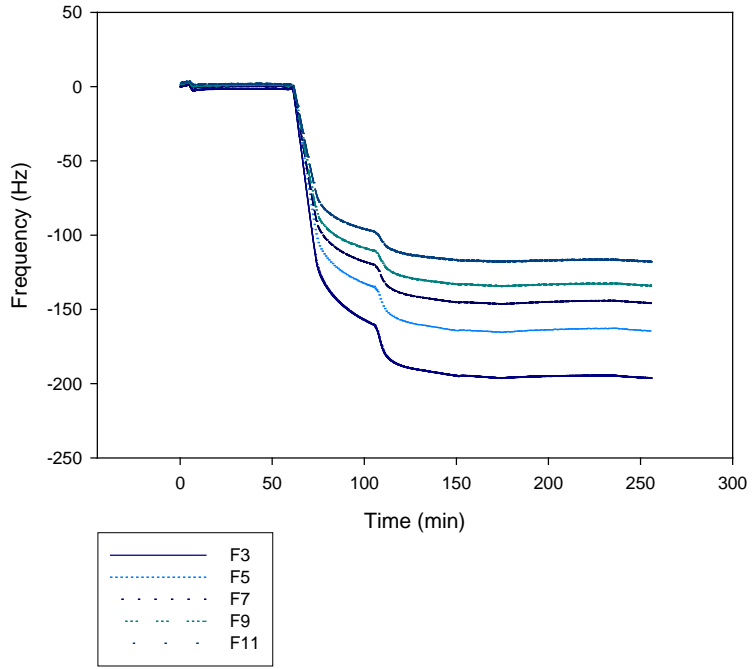
SM(PEG)$_{12}$ Trial 5 Chamber 4

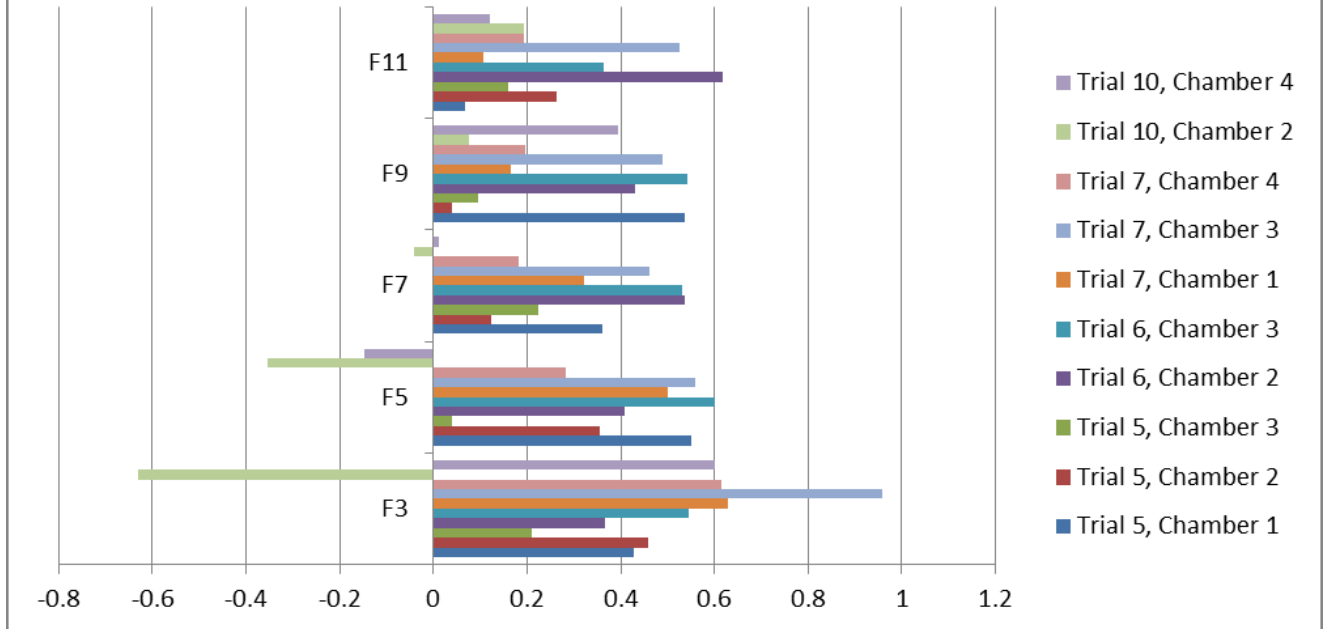**Appendix C: Frequency Changes Due to Peptide and Bacterial Adsorption**

Physically Adsorbed Chrysophsin-1
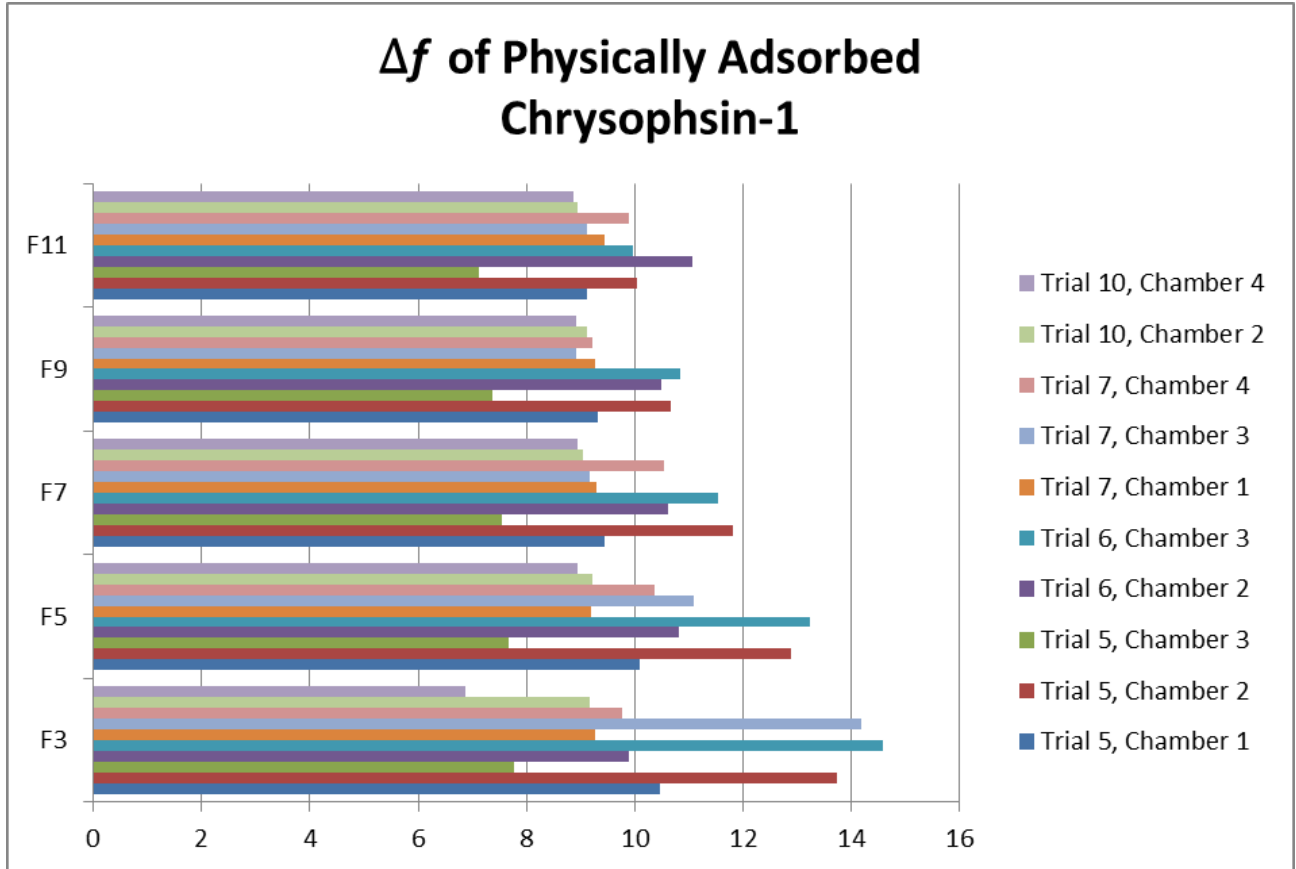
Δ*f* of *S. aureus* Adsorption for Physically Adsorbed Chrysophsin-1

Legend:
- Trial 10, Chamber 4
- Trial 10, Chamber 2
- Trial 7, Chamber 4
- Trial 7, Chamber 3
- Trial 7, Chamber 1
- Trial 6, Chamber 3
- Trial 6, Chamber 2
- Trial 5, Chamber 3
- Trial 5, Chamber 2
- Trial 5, Chamber 1

C-chrysophsin-1 Bound via an SM(PEG)$_{12}$ Linker

Δf of C-chrysophsin-1 bound via an SM(PEG)12 linker

Legend:
- Trial 5, Chamber 4
- Trial 5, Chamber 3
- Trial 5, Chamber 2
- Trial 5, Chamber 1
- Trial 2, Chamber 2
- Trial 2, Chamber 1
- Trial 1, Chamber 2
- Trial 1, Chamber 1
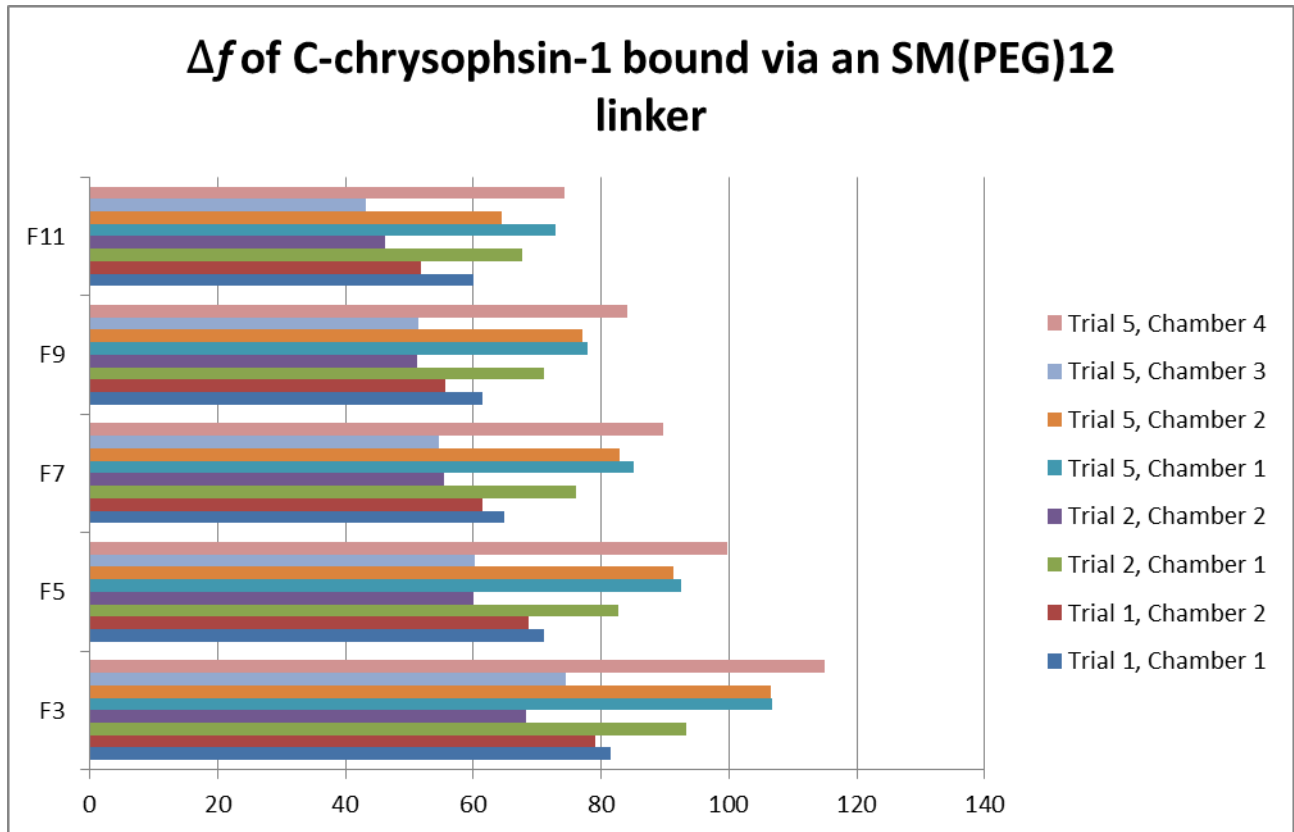
Δ*f* of *S. aureus* Adsorption for
C-chrysophsin-1 bound via an SM(PEG)12 linker

Legend:
- Trial 5, Chamber 4
- Trial 5, Chamber 3
- Trial 5, Chamber 2
- Trial 5, Chamber 1
- Trial 2, Chamber 2
- Trial 2, Chamber 1
- Trial 1, Chamber 2
- Trial 1, Chamber 1
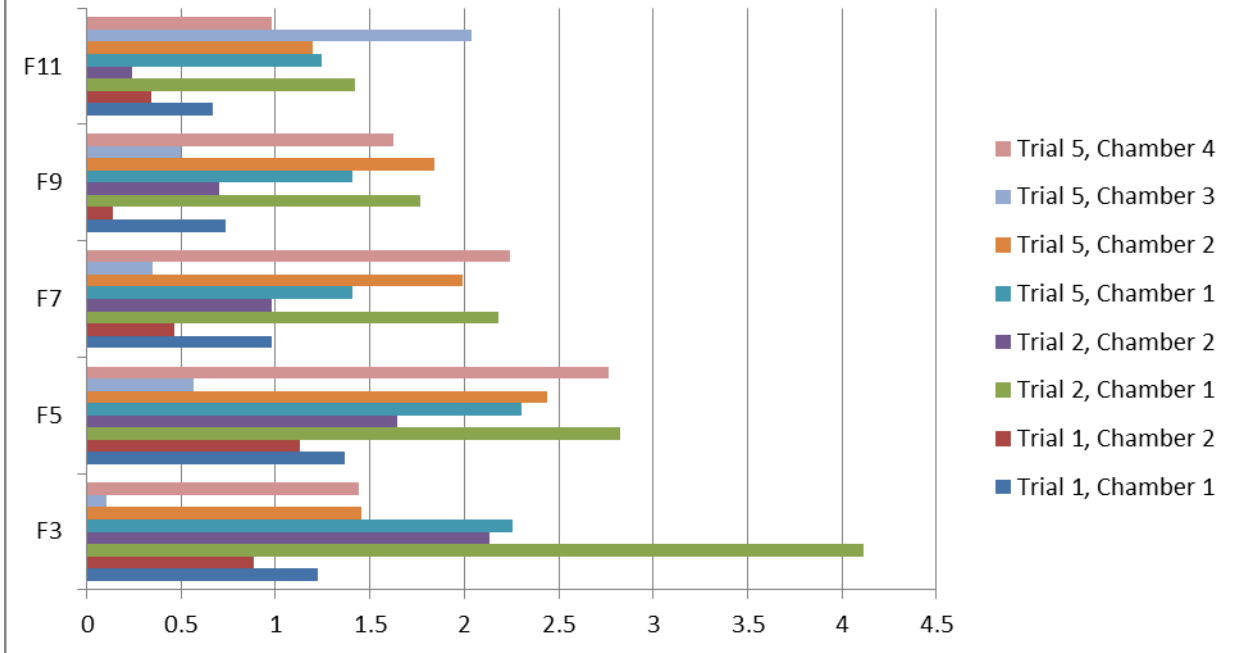
Appendix D: Live/Dead Bacterial Viability Assay Data

Physically Adsorbed Chrysophsin-1

Trial 5	Average	Stdev
Chamber 1	50%	6%
Chamber 2	58%	6%
Chamber 3	43%	11%

Trial 6	% Dead	Stdev
Chamber 2	68%	28%
Chamber 3	73%	19%

Trial 7	% Dead	Stdev
Chamber 1	52%	17%
Chamber 3	49%	15%
Chamber 4	50%	10%

Trial 10	Average	StDev
Chamber 2	50%	12%
Chamber 4	53%	14%

C-chrysophsin-1 Bound via an SM(PEG)$_{12}$ Linker

Trial 1	Average	StDev
Chamber 1	29%	11%
Chamber 2	34%	11%
Overall	32%	11%

Trial 2	Average	StDev
Chamber 1	40%	9%
Chamber 2	37%	8%
Chamber 3	33%	4%

Trial 5	Average	StDev
Chamber 1	34%	11%
Chamber 2	50%	11%
Chamber 3	39%	7%
Chamber 4	48%	11%